Separation and Purification Technology 279 (2021) 119756

Contents lists available at ScienceDirect

Separation and Purification Technology

journal homepage: www.elsevier.com/locate/seppur

Facile fabrication of Anti-biofouling polyaniline ultrafiltration membrane by green citric acid doping process

Elif Gungormus, Sacide Alsoy Altinkaya *

Izmir Institute of Technology, Department of Chemical Engineering, Gulbahce, Urla 35430, Izmir, Turkey

ARTICLE INFO

Keywords:
Citric acid
Polyaniline membrane
Antibacterial property
Antibiofouling
Green doping process

ABSTRACT

This study aimed to enhance the anti-biofouling property of the polyaniline (PANI) based ultrafiltration (UF) membrane by utilizing its self-acid doping ability. A naturally derived biodegradable agent, citric acid, was doped to the membrane by filtering at 1 bar. Acid doping increased the hydrophilicity, made the surface nearly electroneutral, and imparted biocidal characteristics to the membrane. Biofouling was simulated by filtering a suspension of E.coli and S.aureus through the membranes. Most fouling on the doped membrane was reversible and easily removed by simple washing, leading to a high flux recovery ratio. The SEM images taken after filtration and washing steps showed that the modified membrane surface was free of bacteria while many bacteria accumulated on the pristine membrane surface. The doped membrane was stored in 1 M NaCl solution for up to five months. A tiny amount of citric acid was lost from the membrane, and at the end of storage, the flux, rejection, and antibacterial activity values did not change, demonstrating the antibacterial agent's stability. The protocol proposed in this study is fast, simple, facile, and easily scalable for large-scale production. Using a green antibacterial agent and its loading with a one-step process without consuming chemicals or functionalizing the support makes the proposed method environmentally friendly.

1. Introduction

Biofouling is a commonly encountered problem in the environmental applications of membrane technology. Biological fouling, which accounts for more than 45% of all membrane fouling [1], results from bacterial colonization on the membrane surface [2,3]. Severe adverse effects such as reduction in fluxes, increase in energy consumption, decrease in permeate water quality, and eventually, premature replacement of membranes are some of the consequences of biofouling. Currently, pretreatment of feed or aggressive cleaning procedures to reduce and remove biofouling are not preferred solutions due to the self-replicating nature of biofouling organisms and damage to the membrane. Unlike these options, new membrane development or modification of existing membranes is accepted as the primary strategy towards reducing biofouling.

Membrane modification is carried out to achieve anti-biofouling activity through enhancing anti-adhesion and antibacterial properties. Electrostatic repulsion between the membrane surface and foulant both carrying the same charge prevents the adhesion of the foulant on the membrane surface. However, not all foulants in water are completely negatively or positively charged [4-6]. A negatively charged membrane surface becomes unsuitable for treating water containing positively charged foulants or vice versa. To achieve high anti-adhesion properties against both positively and negatively charged foulant molecules, neutrally charged surfaces are highly preferred [7]. Additionally, hydrophilic, and smooth surfaces have less fouling tendency. Zwitterionic polymers combine charge neutrality and high hydrophilicity to obtain an anti-adhesive membrane surface. Researchers have made efforts to use different zwitterionic polymers to improve the anti-biofouling properties of membranes [8-19]. To date, zwitterionic polymer-based membranes have been prepared by using redox-initiated graft polymerization [8], UV graft polymerization [9], photografting [10], and surface initiated atomic transfer radical polymerization [11,19]. These methods require high energy; besides, zwitterionic monomers are expensive, resulting in a significant increase in membrane fabrication cost. Furthermore, achieving uniform polymerization on a large surface area is highly challenging. The anti-adhesive membranes can only control the bacteria attachment and the rate of early biofilm formation. Mitigating bacteria growth and proliferation for a while is only possible with antibacterial membranes since these membranes can attack,

* Corresponding author.
E-mail address: sacidealsoy@iyte.edu.tr (S. Alsoy Altinkaya).

https://doi.org/10.1016/j.seppur.2021.119756
Received 22 June 2021; Received in revised form 1 September 2021; Accepted 15 September 2021
Available online 20 September 2021

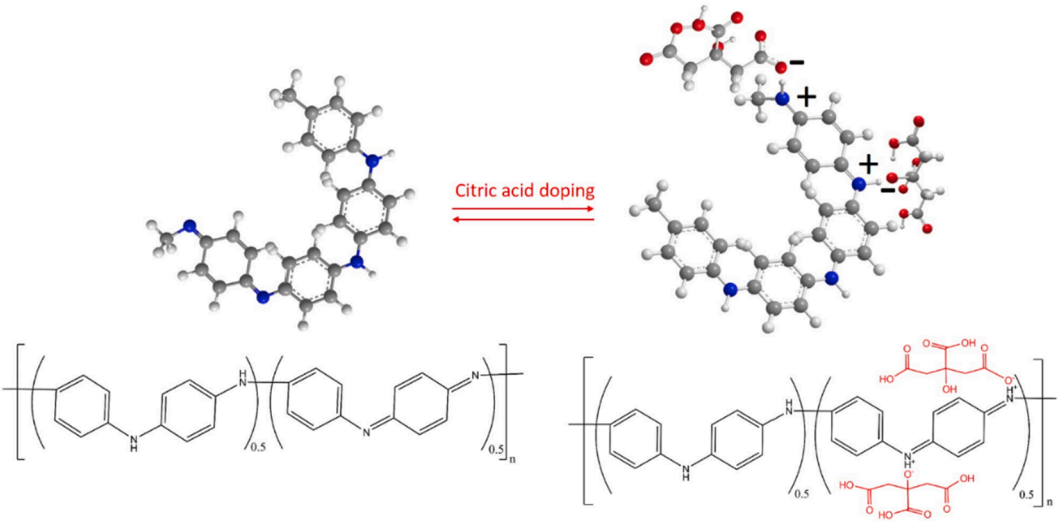

Scheme 1. Rearrangement reaction mechanism between the emeraldine base (EB) and emeraldine salt (ES) polymers through citric acid doping and dedoping in alkaline medium.

disperse, or suppress the activity of attached organisms. Antibacterial functionalization of the membranes was commonly carried out with nanoparticles (e.g., silver, copper, TiO_2, ZnO, MgO). The modified membranes showed their antibacterial action through the continuous release of the nanoparticles [20-24]. This release-killing mechanism causes a shorter lasting period for antibacterial action and raises concern about environmental health. Recently metal–organic frameworks and carbon-based nanomaterials (carbon nanotubes, graphene oxide (GO), and carbon dots) have been used to impart antibacterial activity to the membranes [25-32]. Among these materials, GO has especially received significant attention due to its physicochemical properties, including sheet morphology, size/size distribution, oxygen-containing group density, electronic mobility, and carbon radicals which can substantially impact its antimicrobial activity. Nevertheless, despite its favorable antibacterial property with contact-killing properties, for the moment, procedures for graphene synthesis are time-consuming. They cannot readily produce defect-free samples in large quantities with high yields [33]. In many studies, functionalization of membrane surfaces with positively charged quaternary ammonium compounds (QACs) has been shown to produce stable and long-lasting antibacterial activities [2,3,34-40]. Different QACs have been introduced into membranes through blending during fabrication [2,3,34,35,41], graft polymerization [27,36-40] and coating on the membrane surface [42]. Grafting and coating methods require abundant chemical usage, extensive procedures [27,36-40,42] and may cause a change in the bulk and surface properties [27,39]. In a recent study, we proposed a facile approach for preparing antibacterial polysulfone-sulfonated polyethersulfone (SPES) based ultrafiltration membrane [43]. QAC, added in the coagulation bath, made strong electrostatic interaction with the negatively charged functional groups of the SPES at the membrane surface, hence, provided high antibacterial activity. The only drawback of the QACs is their hydrophobic nature. Although progress has been made, there is still a need for alternative methods/materials which are scalable and cost-effective for large-scale industrial production of ultrafiltration (UF) membranes possessing both anti-adhesion and antibacterial properties. Also, sustainable development goals impose demands on new, innovative, and green solutions for membrane production.

In this study, a new type of anti-biofouling polyaniline (PANI) UF membrane was developed via a facile, simple, and fast route with citric acid doping under dynamic conditions. The most attractive feature of PANI comes from its self-doping ability by protonic acids [44]. Among various acids, citric acid was chosen due to its well-known antibacterial activity [45-47]. It was doped to the membrane through a simple filtration step at low pressure. Citric acid doping protonates the imine groups of PANI and produces positively charged nitrogen [48]. The protonated groups are ionically bound to the negatively charged counter-ion, $C_6H_7O_7^-$, [49]; thus, the polymer backbone becomes electroneutral (Scheme 1). Also, the integration of carboxyl and hydroxyl functional groups to the structure through acid doping increases the hydrophilicity of the resulting membrane. Thus, the PANI membrane modified with citric acid acts like a zwitterion displaying anti-adhesive and antibacterial properties. To date, only a few studies reported the usage of PANI in the development of antibacterial water treatment membranes. In these studies, PANI was used either as a filler in the membrane casting solution [50] or a grafting layer on the commercial reverse osmosis membrane [51]. The antibacterial property was imparted through in situ silver reduction after dopamine coating [50] or copper nanoparticle coating [51]. Both studies utilized many steps and long procedures to prepare the membranes which limit the application of protocols in large scale. The scalability of a membrane production protocol depends on factors such as availability of all materials in large quantities, energy consumption, number of steps, necessity for post treatment or pretreatment, need for harsh chemicals/conditions etc. These factors are closely related with economic considerations where the main motivation is to minimize unit production cost. Herein, we used the PANI as the main membrane polymer that can be synthesized using low-cost monomers and has high thermal, chemical stability, and a hydrophilic structure [52]. We enhanced its anti-biofouling property through citric acid doping. The proposed doping method is a green solution since the citric acid is a naturally derived, water-soluble antibacterial agent and it also has a low cost. Additionally, there is no need either for the post-treatment of the pristine membrane or crosslinking agent for acid doping. Membrane modification by filtration of citric acid can be implemented in large-scale using commercially available dead end or cross flow filtration units (manufactured by Pall Corporation, Fluence Corporation, Salher etc). Overall, the proposed membrane fabrication technique is fast, simple, facile, and can easily be scaled up for large-scale production.

2. Materials and methods

2.1. Materials

The most commonly used form of PANI, the emeraldine base (EB) form, was synthesized using aniline (Sigma-Aldrich, ACS reagent, ≥99.5% purity), ammonium persulfate ($(NH_4)_2S_2O_8$, Sigma-Aldrich,

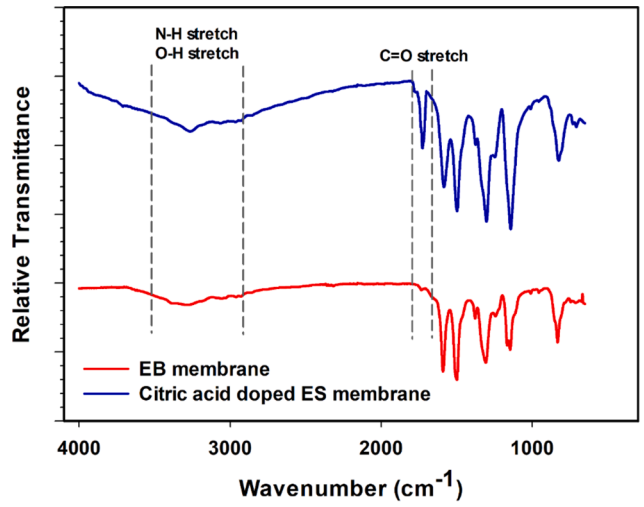

Fig. 1. ATR-FTIR spectra of EB membrane* and citric acid doped ES membrane. *Reprinted from Chemical Engineering Journal, Vol. 389, E. Gungormus, S.A. Altinkaya, "A high-performance acid-resistant polyaniline based ultrafiltration membrane: Application in the production of aluminium sulfate powder from alumina sol". Page 124393, Copyright (2020), with permission from Elsevier.

ACS reagent, ≥98% purity), HCl fuming 37% (Merck), 25% ammonia solution (NH_4OH, Merck), and methanol (Sigma-Aldrich, ACS reagent, ≥99.8% purity). Triethylamine (Riedel-de Haën) and N-methyl-2-pyrrolidone (NMP, Merck, anhydrous, greater than 99.5%) used as gel inhibitor and solvent were utilized in the preparation of membrane casting solution. Molecular weight cut-off (MWCO) of the membranes were determined by using polyethylene glycol (PEG) 1000, 4000, 6000, 10000, and 20000 Da (Sigma Aldrich). The citric acid (ACS reagent, ≥99.5% purity) was purchased from Sigma-Aldrich for the membrane doping process. Gram-negative (Escherichia coli, ATCC 25922) and Gram-positive (Staphylococcus aureus, RSKK 1009) bacteria were used for antibacterial and anti-biofouling tests. NaCl for stability test and phosphate-buffered saline for the antibacterial and anti-biofouling test were purchased from Sigma-Aldrich.

2.2. Polymer synthesis

The EB form of PANI was prepared by chemical oxidative polymerization of aniline. The procedure was adapted from the studies conducted by Ibrahim [53] and Gomes and Oliveira [54]. The oxidizing agent and monomer were separately dissolved in a 1 M HCl aqueous solution, and the resulting solutions were mixed at 0℃. The mixture was first stirred at 0℃ for 4 hr and then at 25℃ for 20 hr. After 24 hr of reaction, the emeraldine hydrochloride precipitate was collected, washed, and filtered to remove unreacted chemicals. The filtered precipitate was treated with 1 M NH_4OH solution to form EB, washed with DI water, and then DI water: methanol mixture and refiltered. Finally, the EB powder was collected and vacuum dried. The detailed procedure was described in our previous study [55].

2.3. Membrane fabrication and modification

The membrane casting solution was prepared by dissolving 15 wt% EB in a mixture of 1.5 wt% trimethylamine and 83.5 wt% NMP. The mixture was homogenized by stirring for one hr at 300 rpm (T = 25 °C), degassed, then cast on a polyester nonwoven fabric (Type TH, Hirose Paper Mfg. Co. Ltd.) with the help of an automated film applicator (Sheen Instrument Ltd., model number: 1133 N). The casted solution was immersed in a coagulation bath (DI water, 20℃) to induce phase inversion and kept in DI water for 24 hr to complete phase separation. The prepared EB membranes were first compacted at 2 bar and then doped with citric acid by filtering aqueous acid solution (pH = 3) at 1 bar for 4.5 hr until reaching a constant flux. The doped membrane will be referred to as citric acid doped ES membrane.

2.4. Membrane performance tests and characterization

The chemical structures of the dried pristine and citric acid doped ES membranes were determined with Attenuated Total Reflectance Fourier Transform Infrared Spectrometer (ATR-FTIR, Perkin Elmer) at ambient temperature over a scanning range of 650–4000 cm^{-1} with a resolution of 4.00 cm^{-1}. A scanning electron microscope (FEI Quanta 250 FEG) and energy dispersive X-ray analysis (EDX) were used for characterizing the surface and bulk morphology of the membranes and for determining the elemental compositions on the membrane surface. The samples were fractured in liquid nitrogen and coated with a thin layer of gold before the analysis. Atomic force microscopy (AFM) images with a 2 μm × 2 μm scanning area were taken in tapping mode to evaluate the surface roughness of the membranes (AFM/SPM MMSPM Nanoscope 8 Bruker). Membrane hydrophilicity was characterized by measuring dynamic contact angles of dried membrane surfaces with a 5 μL of a deionized water droplet (Attension Optical tensiometer). The zeta potentials of the pristine and acid doped membranes were measured in 10 mM NaCl solutions at the pH ranges from 3 to 9 at 25℃ (NanoPlus Micromeritics). Thermogravimetric analysis (TGA) was carried out by using a Setaram, Labsys, TG-DTA/DSC to determine the amount of citric acid doped to the membrane. The heating rate was adjusted to 10℃/min from 25℃ to 900 ℃ under the nitrogen atmosphere.

Performances of the membranes were evaluated by measuring pure water permeability (PWP) and rejection of different-sized PEGs (1000, 4000, 6000, 10000, and 20000 Da). Filtration experiments were carried out by using a dead-end cell filtration system with an effective surface area (A) of 13.4 cm^2 (Millipore, Amicon Stirred Cell 50 ml). The membranes were first compacted until reaching steady-state condition. Following compaction, the permeate volume (ΔV) was measured over a specific time period (Δt) at the transmembrane pressure (ΔP) of 1 bar. The PWP and water flux (J_W) were then calculated by using Eq. (1).

$$PWP = \frac{\Delta V}{A \times \Delta t \times \Delta P} = \frac{J_W}{\Delta P} \quad (1)$$

The PEG rejection (R, %) was calculated from Eq. (2) using the PEG concentrations of the feed (C_F:1 g/L), permeate (C_P) and retentate (C_R) streams measured with Rudolph-J357 Automatic Refractometer.

$$R(\%) = \left(1 - \frac{C_P}{0.5 \times (C_F + C_R)}\right) \times 100 \quad (2)$$

The pore size distribution of the membranes was estimated from Eq. (3) using the two-parameter log-normal distribution function [39,56-58] with the assumptions of no interaction (steric and hydrodynamic) between the neutral PEG molecules and pores of the membranes [39,58]:

$$\frac{dR(r_p)}{dr_p} = \frac{1}{r_p ln(\sigma_p)\sqrt{2\pi}} exp\left[-\frac{1}{2}\left(\frac{ln(r_p/\mu_p)}{ln(\sigma_p)}\right)^2\right] \quad (3)$$

where the geometrical mean radius of the solute (μ_p) was obtained at R = 50% and the geometrical standard deviation of the solute (σ_p) was defined as the ratio of r_p of R = 84.13% to that of R = 50%. The radii of PEG were predicted from Eq. (4), which was derived from Stokes-Einstein law by assuming a spherical particle [59].

$$r_p = 16.73 \times 10^{-12} \times MW^{0.557} \quad (4)$$

where the unit of molecular weight (MW) is Da.

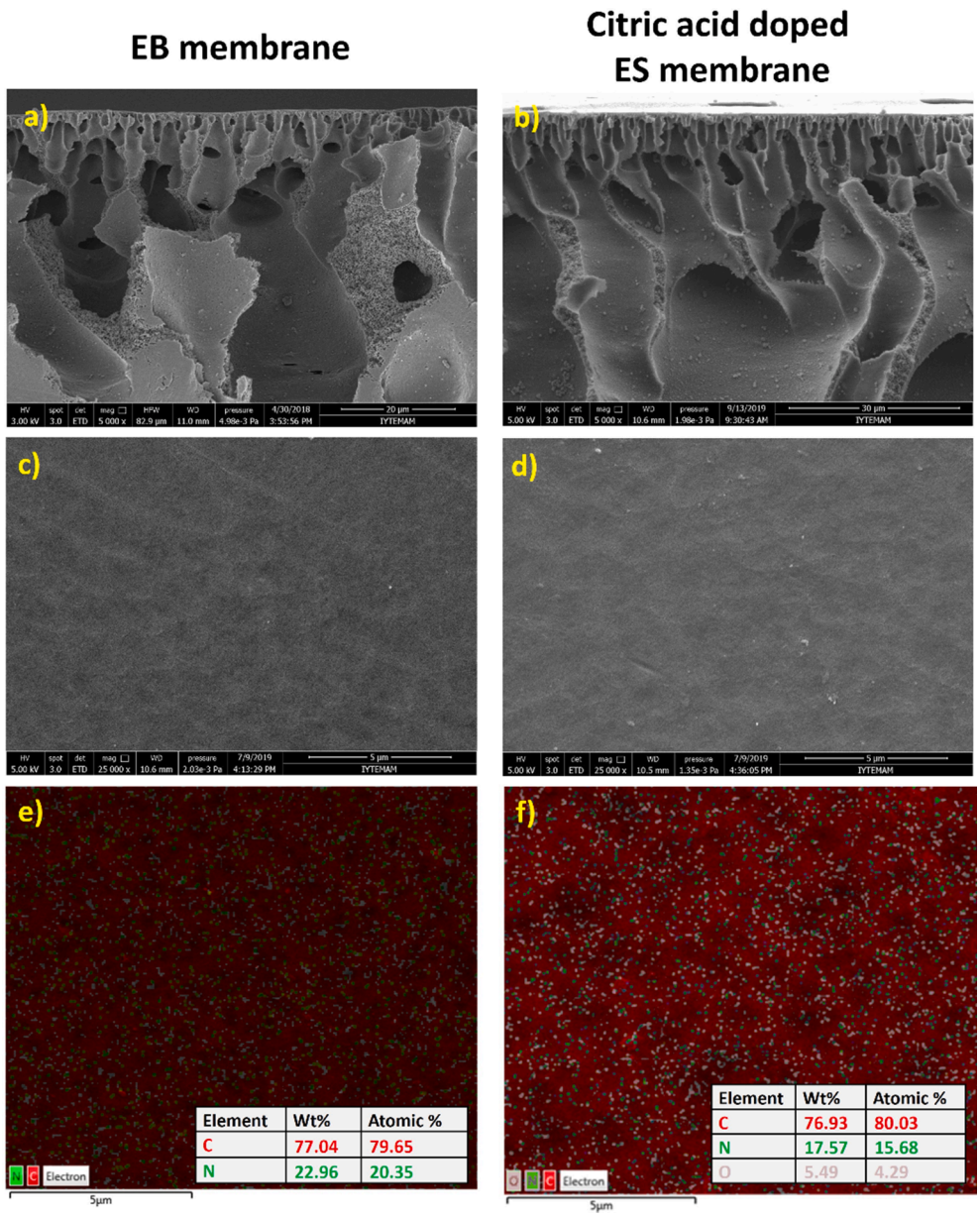

Fig. 2. SEM cross-sectional images, surface images, and EDX elemental analysis of the EB membrane and the citric acid doped ES membranes.

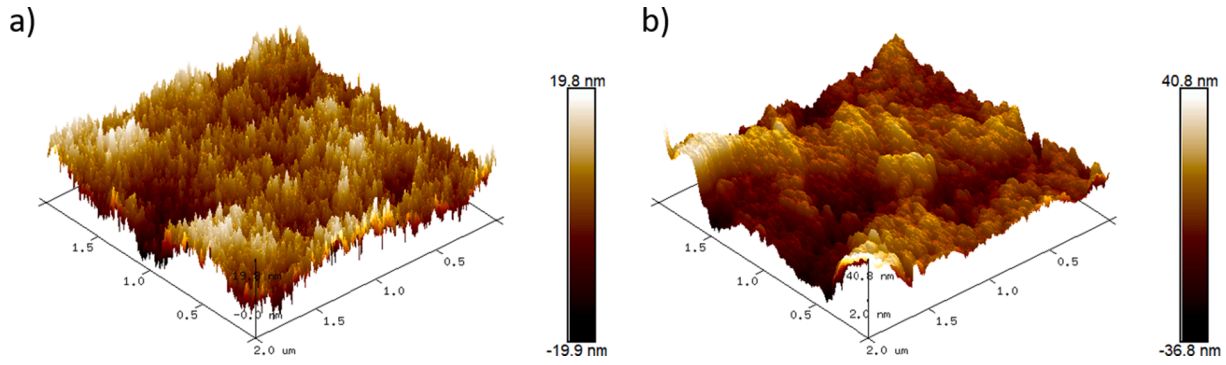

Fig. 3. AFM images of the a) EB membrane* and b) citric acid doped ES membrane. *Reprinted from Chemical Engineering Journal, Vol. 389, E. Gungormus, S.A. Altinkaya, "A high-performance acid-resistant polyaniline based ultrafiltration membrane: Application in the production of aluminium sulfate powder from alumina sol". Page 124393, Copyright (2020), with permission from Elsevier.

Table 1
Properties of the prepared membranes.

	EB membrane	Citric acid doped ES membrane
R_a (nm)	2.67	4.59
R_q (nm)	3.36	5.74
Contact Angle (°)	76.22 ± 0.85	59.41 ± 0.85
PWP ($Lm^{-2}hr^{-1}bar^{-1}$)	97.57 ± 1.53	52.62 ± 0.74
MWCO (Da)	7500	6600
Pore **radius**(95th percentile, nm)	2.89	2.52

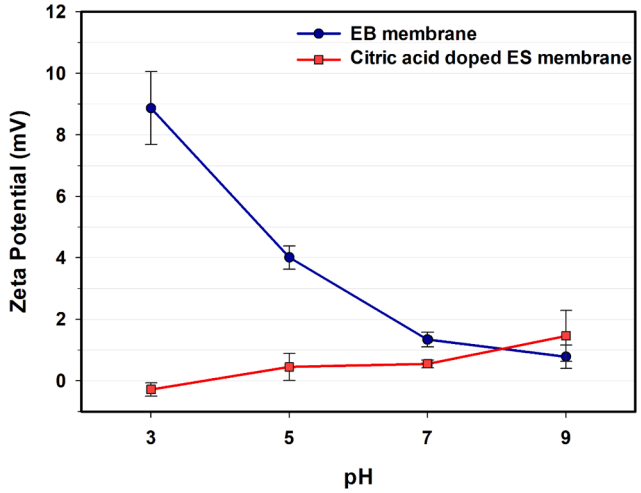

Fig. 4. Zeta potential as a function of pH for the EB membrane and citric acid doped ES membrane.

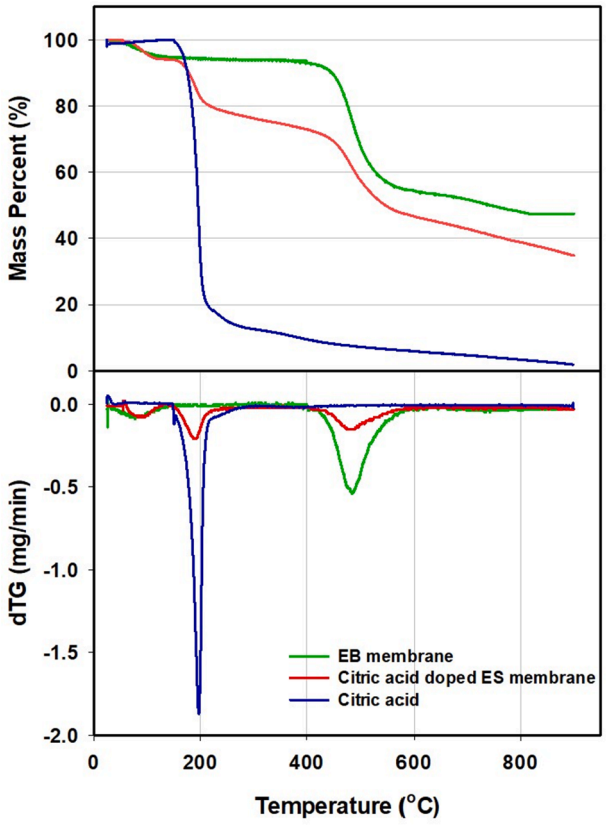

Fig. 5. TGA and dTG (derivative thermogravimetry) analysis of citric acid, EB membrane, and citric acid doped ES membrane.

2.5. Antibacterial activity tests

The antibacterial activities of the membranes were determined according to ASTM E2180 standard protocol. E.coli and S.aureus cells, used as model Gram-negative and Gram-positive bacteria, were incubated in nutrient agar and soy agar, respectively, for 24 hr at 37 °C up to reaching exponential growth phase of bacteria. Bacterial suspensions were prepared in 0.1% (w) peptone water with a concentration of 0.5 McFarland, then diluted with nutrient and soy broth to obtain final concentrations of 3.5×10^6 and 4.2×10^6 CFU/mL for E.coli and S. aureus, respectively. The membrane coupons (active surface area: 3 cm × 3 cm) were sterilized with UV for 30 min and then placed into Erlenmeyer flasks. Each membrane coupon was incubated in the bacterial solution (300 μL) for either 1 hr or 24 hr at 37 °C. Following incubation, 50 ml phosphate-buffered saline solution (PBS, pH = 7.4) was added to the Erlenmeyer flask, which was subjected to 10 min bath sonication to remove bacteria attached to the membrane coupon. The obtained E.coli and S.aureus suspensions were spread on plates including nutrient agar and soy agar, respectively, incubated for 24 hr at 37 °C, and finally, the colonies on the plates were counted. All samples were analyzed in quintuplicate.

The reduction rate of the bacteria was calculated from the following equation by counting the number of colonies on the agar plate after contacting with the pristine (N_{EB}) and citric acid doped (N_{ES}) membranes.

$$\text{Reduction Rate } (\%)) = \frac{N_{EB} - N_{ES}}{N_{EB}} \times 100 \quad (5)$$

2.6. Antibiofouling performance tests

Antibiofouling performance tests were carried out using a dead-end filtration cell (effective membrane area 13.4 cm^2). The concentrations of E.coli and S.aureus suspensions in PBS (pH = 7.4) were adjusted to $1.75x10^8$ and $2.1x10^8$ CFU/mL, respectively. Membranes were sterilized with UV light for 20 min. Following compaction at 2 bar, the initial pure water fluxes of both membranes (J_W) were adjusted to similar values (about 50 L/m^2hr). Next, 250 ml of *E.coli* and *S.aureus* solutions were filtered through pristine and acid-doped membranes. The treated membranes were rinsed with PBS for 10 min, and pure water fluxes were remeasured (J_R). This cycle was repeated for 5 times. The flux recovery ratio (FRR) was then calculated from

Table 2
The PWP of commercial membranes with comparable *MWCO* manufactured by different companies.

Supplier	Code	*MWCO*	Polymer Type	Permeability($Lm^{-2}hr^{-1}bar^{-1}$)
Millipore Ultracel	PLC5	5000 Da	Regenerated Cellulose	14.5
	PLCC	5000 Da	Regenerated Cellulose	21.8
Sartorius	RC	5000 Da	Regenerated Cellulose	20
	PES	5000 Da	Regenerated Cellulose	20
TriSep™	UF5	5000 Da	Polyethersulfone	12
	UF10	10000 Da	Polyethersulfone	74
Microdyn™	UP005	5000 Da	Polyethersulfone	10
	UP010	10000 Da	Polyethersulfone	50
Synder™	ST	10000 Da	Polyethersulfone	65–83

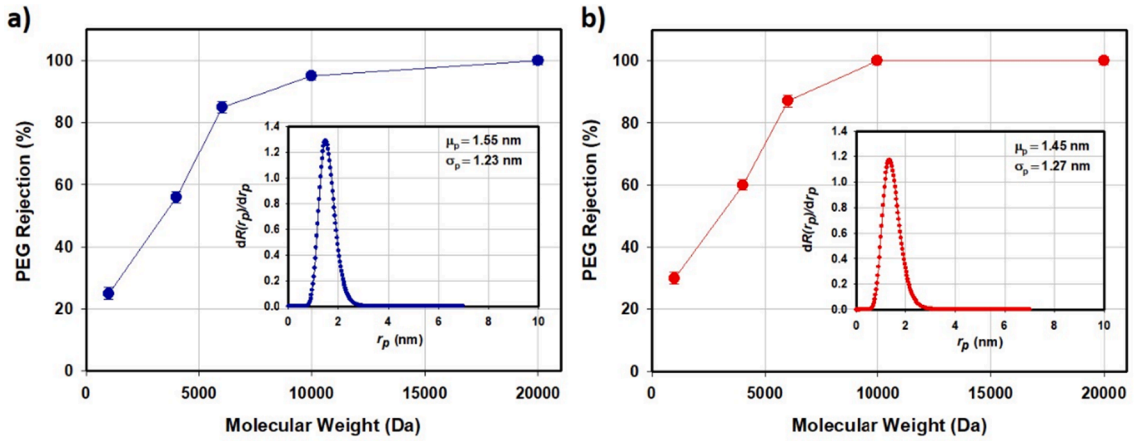

Fig. 6. The *MWCO* of the a) EB membrane and b) citric acid doped ES membrane.

$$FRR(\%) = \frac{J_R}{J_W} \times 100 \quad (6)$$

The antifouling property of the membrane was further evaluated by determining reversible fouling (R_r), and irreversible fouling (R_{ir}) resistances, calculated in Eq. (7) and Eq. (8).

$$R_r(\%) = \frac{J_R - J_P}{J_W} \times 100 \quad (7)$$

$$R_{ir}(\%) = \frac{J_W - J_R}{J_W} \times 100 \quad (8)$$

where J_P is the flux of bacteria suspension passing through the membrane.

The surface images of unmodified and citric acid doped membranes after **1st cycle** bacteria filtrations were taken by using SEM (FEI Quanta 250 FEG).

2.7. Stability test for the citric acid doped ES membrane

The stability of the citric acid doped ES membrane was tested by storing in 1 M NaCl solution (25 °C) for up to 5 months. To this end, the concentration of citric acid in the solution was measured with Total Organic Carbon (TOC) analyzer (Shimadzu TOC-Vcph (TNM-1/SSM-5000A). The results were reported as % of citric acid released into storage medium with respect to its initial amount loaded to the membrane. Additionally, the PWP and rejection of the membrane (with PEG 6000 Da) were determined. Furthermore, the antibacterial activity of the citric acid doped ES membrane at the end of 1-month storage in 1 M NaCl solution (25 °C) was also determined according to ASTM E2180 standard protocol with the same antibacterial activity test conditions mentioned in Section 2.5.

3. Results and discussion

3.1. Effect of citric acid doping on the structure, chemical composition, and surface properties of the EB membrane

The FTIR spectra of EB membrane and citric acid doped ES membrane are shown in Fig. 1. The typical peaks for nitrogen quinoid and benzenoid were found at 1600 and 1500 cm^{-1}, respectively [60]. The C–N stretch of a secondary amine group was observed at 1300 cm^{-1}, and the aromatic C–H in-plane bending modes were originated in the region of 1010–1170 cm^{-1} [61-63B–D]. A new peak appeared at the band of 1729 cm^{-1} due to the C = O stretching [64,65] and increased band width at 3400 cm^{-1} due to the stretching frequencies of OH and NH groups [66] proved citric acid doping to the membrane.

Fig. 2 shows the cross-section and surface images of the membranes, including EDX-SEM mapping for carbon, nitrogen, and oxygen. Both pristine and citric acid doped membranes showed a typical asymmetric membrane structure consisting of a thin, dense skin top layer and a porous sublayer with finger-like macrovoid morphology, as shown in Fig. 2.a and 2.b. The acid doping in the porous sublayer did not change the bulk structure due to the small size of the citric acid. Also, surface structures of the pristine and doped membranes were found similar (Fig. 2.c and 2.d). The EDX analysis confirmed the successful citric acid doping by detecting oxygen only in the ES membrane (Fig. 2.f). In addition, the C:N ratio (atomic-based) increased from 3.91 to 5.10 upon doping (Fig. 2.e and Fig. 2.f).

The EB membrane exhibited a comparatively uniform ridge-and-valley morphology (Fig. 3.a), while the ES membrane demonstrated a plating structure with a relatively rough surface (Fig. 3.b). The roughness parameters (R_a and R_q) were determined as 2.67 nm and 3.36 nm for the EB membrane [55]; 4.59 nm and 5.74 nm for the citric acid doped ES membrane (Table 1). Citric acid doping enhanced the hydrophilicity of the EB membrane as confirmed by the decrease of the contact angle from 76.22 ± 0.85° [55] to 59.41 ± 0.85°. The enhanced hydrophilicity is due to the hydrophilic carboxyl and hydroxyl functional groups of citric acid attached to the polymer backbone.

The pristine EB membrane is positively charged at pH 3 and 5 and becomes neutral at pH 7 and 9 [55]. The doped membrane is almost neutral in all pH values, as shown in Fig. 4. The electroneutrality results from the attachment of the negatively charged counter-ion $C_6H_7O_7^-$ to the protonated imino functional groups of PANI (Scheme 1). The deprotonation of the ES membrane at high pH causes the removal of citric acid from the polymer backbone by the OH group, resulting in returning the membrane to the EB form with a higher positive charge density [55].

Fig. 5 shows the TGA curves of both membranes. The EB membrane degraded between 400 °C and 585 °C; finally, the degraded products became carbonized after 585 °C. On the other hand, a new degradation step was detected for the modified membrane from 148 °C to 260 °C. By comparing with the TGA curve of pure citric acid, the weight loss between 148 °C and 260 °C was attributed to the loss of citric acid and was used to calculate citric acid loading in the membrane (16% where 1 m^2 of the 200 μm thick membrane contains 16.53 g of citric acid). The molecular size of citric acid (192 Da) is much smaller than the pore size of the membrane (*MWCO* of the unmodified membrane:7500 Da, see Table 1). As a result, the carboxyl and hydroxyl functional groups of citric acid are attached at the surface and the interior pore walls of the membrane.

The *PWP* and *MWCO* values of the unmodified EB membrane decreased from 97.57 ± 1.53 $Lm^{-2}hr^{-1}bar^{-1}$ and 7500 Da [55] to 52.62 ± 0.74 $Lm^{-2}hr^{-1}bar^{-1}$ and 6600 Da upon citric acid doping (Table 1).

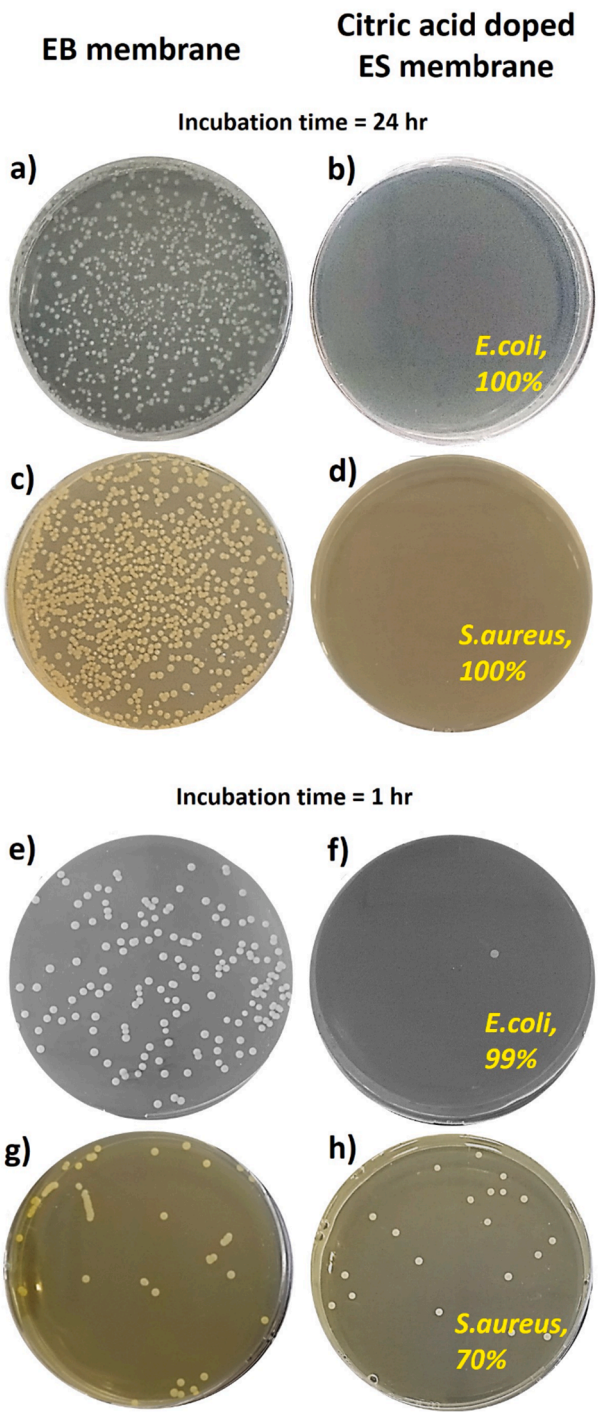

Fig. 7. Bactericidal rates within (a,b,c,d) 24 hr and (e,f,g,h) 1 hr incubation times for the EB and citric acid doped ES membranes (Bacteria suspensions were diluted 100-fold, before spreading on these plates).

Pore size of the membranes can be accurately estimated by choosing the correct model to evaluate the solute rejection data. If the model solutes used in rejection experiments and membrane surface are charged, then, charge-charge interaction should be considered [67]. On the other hand, Causserand et al. [67] reported that when neutral solutes are used and membrane charge density is low, then, the energy of interaction between the solutes and the membrane can be assumed negligible. We used neutral PEGs as model solutes and at the filtration pH, the membranes are almost neutral (zeta potential value at pH = 7: 1.34 ± 0.55 mV for EB membrane and 0.24 ± 0.13 mV for citric acid doped membrane). Therefore, the effect of membrane charge on the pore size calculation was considered negligible. Both the pristine and doped membranes have exhibited higher permeabilities than the commercial membranes with comparable *MWCO* manufactured from different polymers (Table 2). Although citric acid doping enhanced surface hydrophilicity and roughness, the *PWP* decreased after modification. Hydrophilicity increases membrane's water uptake and wettability through enhanced interaction between water molecules and pore wall. On the other hand, since the pore size is on the sub nanometer scale (Table 1), water molecules interact stronger with pore walls resulting in increased friction and reduced flow velocity [68]. Increased surface roughness positively affects the *PWP* by increasing the effective surface area available for permeation of water molecules [69], however, the results showed that the roughness did not have a dominant effect on the permeability. The decrease in the *PWP* was due to reduced pore radius from 2.89 nm to 2.52 nm (95th percentile), as shown in Fig. 6.

3.2. Antibacterial activity of the membranes

Fig. 7 shows the antibacterial activities of the pristine and acid-doped membranes against *E.coli* and *S.aureus*. After 24 hr incubation, the EB membrane did not demonstrate inactivation on both bacteria (Fig. 7.a and 7.c). On the other hand, the citric acid doped membrane exhibited excellent antibacterial activity and achieved 100% bacterial inactivation rates (Fig. 7.b and 7.d). The doped membrane was effective even at a short contact time, killed 99% *E.coli* and 70% *S.aureus* in 1 hr (Fig. 7.f and 7.h). *S.aureus* has a thicker peptidoglycan layer (≈30 nm) consisting of a network of crosslinking carbohydrates and peptides [70]. This layer acts as a barrier to external stresses; thus, 1 hr contact time was not enough for its disruption. Unlike *S.aureus,* the peptidoglycan layer in *E.coli* is thinner (≈ 10 nm) [71], easily disrupted by the ES membrane even in 1 hr contact. The number of bacteria on the EB membrane increased with time (Fig. 7.a, 7.c, 7.e, and 7.g). Table 3 compares the antibacterial activities of different UF membranes against *E.coli* and *S.aureus*. As seen in the table, the initial number of bacteria, incubation time, and membrane area used in these studies vary significantly. A fair comparison of the antibacterial activities is only possible based on the number of bacteria exposed to a 1 cm^2 membrane area. Wang et al. [72,73] reported 100% and 99.93% *E.coli* inactivation rates at the end of 24 hr incubation. However, the initial number of bacteria used in their study was 10 times lower (1.5×10^4 CFU/cm^2 [72] and 2.4 × 103 CFU/cm^2 [73]) than the amount used in our study (11.7×10^4 CFU/cm^2). The inactivation rate of *S.aureus* by different membranes within 24 hr contact varied between 92.6% and 100% [43,74-76]. However, the absence of some critical data such as membrane area or initial bacteria concentration did not allow the comparison of these membrane's performances. We recently developed a polysulfone-sulfonated polyethersulfone UF membrane containing cetyltrimethylammonium bromide (CTAB) as an antibacterial agent [43]. This membrane was tested under the same conditions as the current study and exhibited 100% and 99.9% inactivation of *E.coli and S.aureus*. Zeng et al. [27] observed a higher inactivation rate for *S.aureus* (77.9%) within 1 hr incubation than ours (70%). However, their membrane preparation protocol requires many steps and a large amount of chemical consumption; thus, it cannot be easily scaled up.

3.3. Antibiofouling performance of the membranes

We evaluated the antibiofouling properties of the membranes with 5-cycle dynamic bacteria filtration tests. As seen in Fig. 8, the unmodified EB membrane displayed 70% and 61% flux declines after filtering 935 L/m^2 of *E.coli* and *S.aureus* solutions, respectively. The same filtration scenario resulted in 12% and 21% flux declines for the citric acid doped ES membrane, suggesting that the acid doping provided anti-biofouling property. The flux of the EB membrane decreased continuously during filtration with both bacteria solutions in each cycle. In contrast, the

Table 3
Static antibacterial activity of the UF membranes in the literature.

Membranes	Contact time	Contact area (cm^2)	Volume of bacteria		Bacteria concentration(CFU/mL)		Antibacterialrate (%)		Ref.
			E.coli	*S.aureus*	*E.coli*	*S.aureus*	*E.coli*	*S.aureus*	
PEK-N-Cl	30 min /1 hr	4	20 μL	-	10^6	-	94.6/100	-	[77]
GOQDs-PVDF	1 hr	2	1 ml	1 ml	10^7	10^7	88.9	77.9	[27]
MBHBA/AA-PSF	24 hr	4	100 μL	-	6×10^5	-	100	-	[72]
PVDF/MWNTs-g-CDDAC	24 hr	-	50 μL	-	10^6	10^6	92.7	95.2	[74]
(PA-$CuCl_2$)/PSf	4 hr	4	10 ml	-	10^7	-	99	-	[78]
PS-P4VP-Z	4 hr	-	-	-	10^6	-	73.81	-	[79]
GO-AgNPs	2 hr/4 hr	-	-	-	10^5	-	86/100	-	[80]
N-PPS,N-T-PPS	18 hr	-	3 ml	-	10^5	-	99	-	[38]
PDA-b-PBA	48 hr	-	120 ml	120 ml	10^6	10^6	92.70	81.3	[81]
HPEI-GO/PES	24 hr	-	5 ml	-	10^6	-	74.88	-	[82]
GO-p-PES	3 hr	1.54	100 μL	-	10^5	-	80	-	[33]
Chitosan/BPPO	12 hr	9	10 ml	-	-	-	70	-	[83]
HNTs-CS@Ag/PES	24 hr	-	5 ml	5 ml	10^6	10^6	94	92.6	[75]
MOF-199@PVDF	2 hr	6	100 μL	100 μL	10^6-10^7	10^6-10^7	100	100	[84]
PSf/PES-AM-VT 1.0	24 hr	3	-	-	-	-	92.3	-	[85]
PES/SPSf/GO	18 hr	-	45 ml	-	-	-	90	-	[86]
PSF/GO-Ag	6 hr	6	-	-	10^7	10^7	70.7	61.8	[87]
rGO-ZnO/PES	3 hr	1.13	100 μL	100 μL	10^6	10^6	95	<10	[88]
PVDF–TiO_2/oxine	3 hr	1.77	-	-	10^8	-	greater than60	-	[89]
PLA/TiO_2 nfs-15%	24 hr	0.3[a]	2 ml	2 ml	-	-	95	99.9	[76]
Fe-Al-Mn@chitosan-CA	12 hr	7.5	1 ml	1 ml	10^5	10^5	-[b]	-[b]	[90]
Z-PAEO	8 hr	3.14	20 ml	-	10^6	-	<98	-	[91]
PI-Ag/CM	24 hr				10^5		99	-	[92]
MIL-125(Ti)/PVDF	2 hr	-	100 μL	-	-	-	100	-	[93]
MSH@UiO-66- NH_2-TFN	3 hr	-	-	-	3×10^5	-	-[b]	-	[94]
MQ_{HCMC}	24 hr	9	300 μL	300 μL	3.5×10^6	4.2×10^6	99.84	100	[43]
PSf-g-pMBHBA	24 hr	25	0.1 ml	0.1 ml	6×10^5	-	99.93	-	[73]
CA/LCNF 9	24 hr	-	1 ml	-	10^5	-	47	-	[95]
ZGONH/PES (1.0 wt%)	6 hr	6	10 ml	10 ml	10^6	10^6	81.1	85.7	[96]
EB	24 hr	9	300 μL	300 μL	3.5×10^6	4.2×10^6	-	-	This Study
Citric acid doped ES	24 hr	9	300 μL	300 μL	3.5×10^6	4.2×10^6	100	100	

[a] in the unit of gram
[b] antibacterial rates were not reported

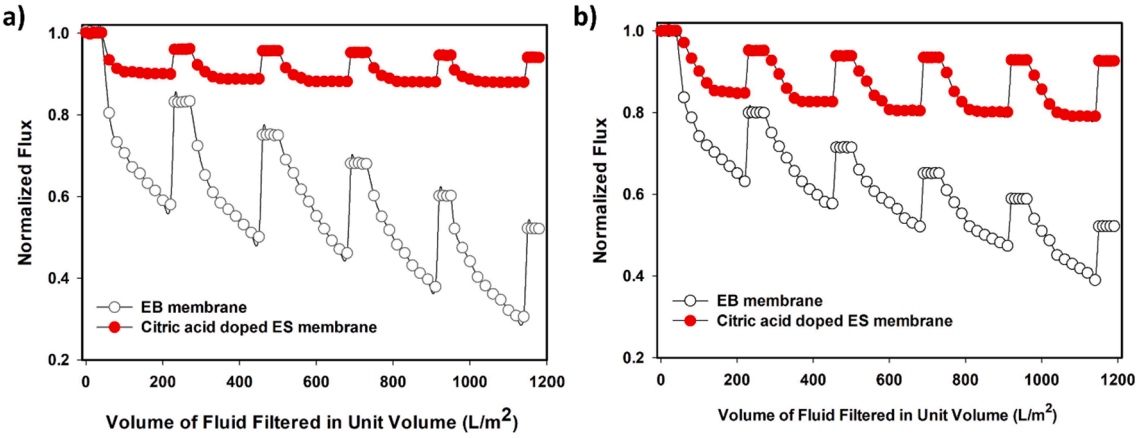

Fig. 8. Normalized flux of the EB membrane and citric acid doped ES membranes as a function of volume filtered per unit area during a) *E.coli* and b) *S.aureus* filtrations. Initial water fluxes of the membranes: ~50 L/m^2hr.

doped ES membrane displayed stable fluxes after the initial drop.

The flux recoveries of the pristine membrane after *E.coli* and *S.aureus* filtration were 52.05 ± 1.09 % and 52.19 ± 1.03 % at the end of the fifth cycle (Fig. 9). The irreversible biofouling on this membrane increased gradually up to about 48% for both *E.coli* and *S.aureus* filtration. Hence, the bacteria colonization on the surface and increased biofilm thickness over time caused the continuous flux decline for the unmodified membrane (Fig. 8). As seen in Fig. 9, the *FRR* for the ES membrane remained constant over 5 filtration cycle. Most fouling on this membrane was reversible and dead bacteria accumulated on the surface were quickly removed after 10 min washing with PBS, resulting in high *FRR* (94.02 ± 1.18% and 92.59 ± 1.10 % at the end of the fifth cycle *E.coli* and *S.aureus* filtrations, respectively).

The accumulation of bacterial population on the pristine EB membrane was clearly observed with SEM pictures, as shown in Fig. 10.a and 10.c. In contrast, the doped membrane surface was free of bacteria (Fig. 10.b and 10.d). The citric acid doping enhanced the surface hydrophilicity, hence, weakened the interaction of bacteria with the surface. Additionally, the nearly net-zero surface charge (Fig. 4) prevented the electrostatic interaction of the bacteria with the surface. Hence, the anti-adhesion property, combined with the high antibacterial activity, improved the biofouling resistance of the doped membrane (Scheme 2). Previous studies also reported higher resistance to cell attachment for hydrophilic, uncharged surfaces [13,97,98].

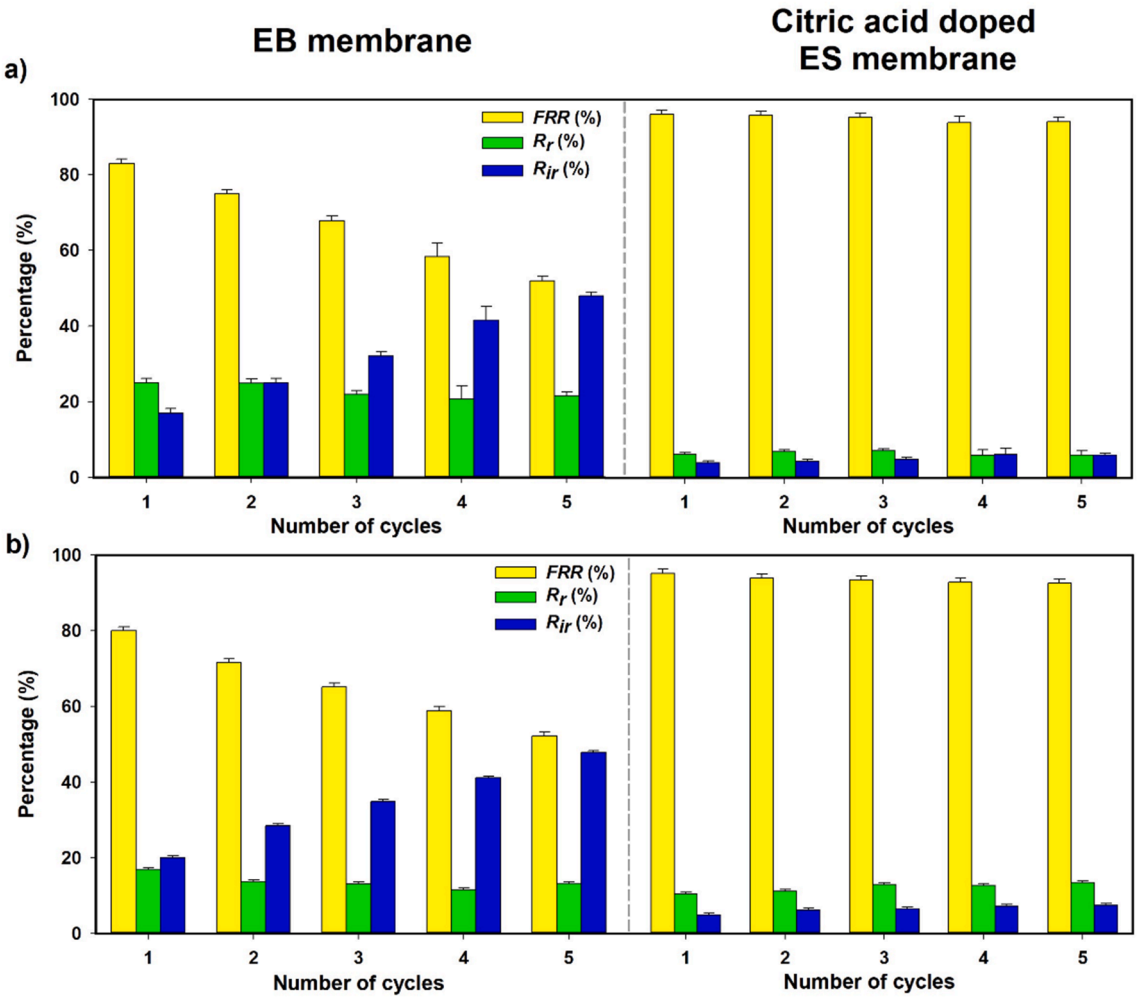

Fig. 9. Flux recovery ratio and biofouling resistances of the membranes during a) *E.coli* and b) *S.aureus* filtrations.

Although many studies tested the biofouling tendency of the membranes with the *E.coli* and *S.aureus* filtration, a fair comparison of the anti-biofouling performances is only possible if the initial fluxes of the membranes are similar. Kim et al. [99] reported reduced flux declines with the decreased initial flux of the silver-containing membrane during the filtration of *E.coli* solution. Given this limitation, we only found one study that used the cross-flow filtration and reported the same initial flux as ours [33]. Although the *E.coli* concentration used in our study was 100 times higher (1.3×10^7 CFU/cm^2) than theirs (4.8×10^5 CFU/cm^2) and we used dead-end filtration, the flux declines observed were found similar (12% in this study and 11.5% in the study of Zhang et al. [33]). In cross-flow, the permeate flux does not drop as fast when compared to dead-end filtration [100]. Thus, our membrane will most probably exhibit even lower flux decline under cross-flow filtration conditions.

Biocidal nanomaterials including silver [21,22,24], copper [20], TiO_2 [101,102], and GO [86,103] are commonly attached to the surface of UF membranes to eliminate biofouling. The synthesis of these nanomaterials requires long preparation steps and the use of harsh chemicals [33,104]. Also, most membranes are first functionalized to attach these antibacterial agents [105,106]. In contrast, the citric acid used in this study can be easily doped through a simple, one-step filtration without any need for the post treatment of the membrane. Furthermore, the citric acid is from natural sources and there is no hazardous waste generated during the doping process. In conclusion, we propose a green + green solution to the current membrane production due to the source of the antibacterial agent and the simplicity of the doping method (Scheme 3).

3.4. Antibacterial stability of citric acid doped ES membrane

Antibacterial membranes kill bacteria through release (release-killing) or direct contact of antibacterial agents with bacteria (contact-killing). We determined the killing mechanism of the citric acid doped membrane in two steps by first determining the amount of citric acid leached from the membrane and then by measuring the antibacterial activity of the leached membrane against *E.coli* and *S.aureus*. The EB membrane contains benzenoid amine and quinonoid imine groups. During doping, the imine groups are preferentially protonated by citric acid [49] resulting in positively charged nitrogen. The ionization product of citric acid, $C_6H_7O_7^-$, then ionically bonds to the positively charged nitrogen as illustrated in Scheme 1. We evaluated the leaching of citric acid by storing the membrane in 1 M NaCl solution which represents a harsh environment since high salt concentration can rupture ionic bond [107]. Fig. 11.a shows that after 5-month storage, a tiny amount, only 1.97% of citric acid loaded to the membrane released into NaCl solution. The leached citric acid consisted of the free acid molecules physically adsorbed to the chains. The released amount did not change between 30 and 150 days, demonstrating the strong bonding of the citric acid to the ES membrane. As shown in Fig. 11.b, the same *PWP* and the rejection values measured within 5 months of storage also confirmed the stability of the doped membrane. After one-month storage in 1 M NaCl solution, the antibacterial activity of the citric acid doped ES membrane against *E.coli* and *S.aureus* did not change (Fig. 12), when

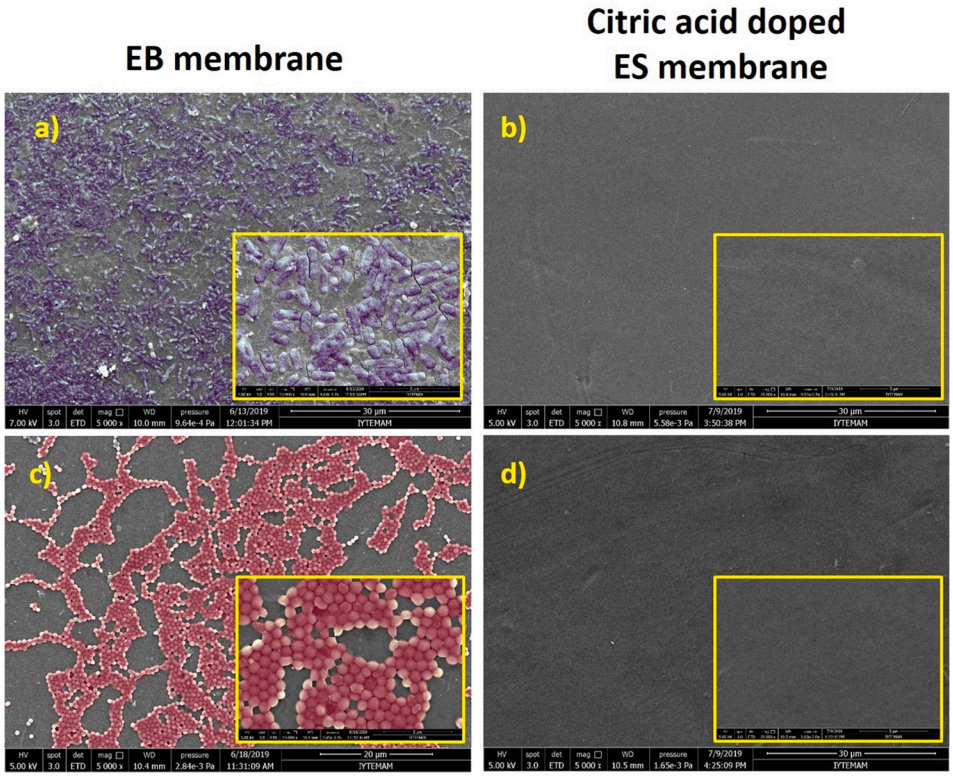

Fig. 10. Surface SEM images of the membranes at the end of **1st cycle** (a,b) *E.coli* and (c,d) *S.aureus* filtrations.

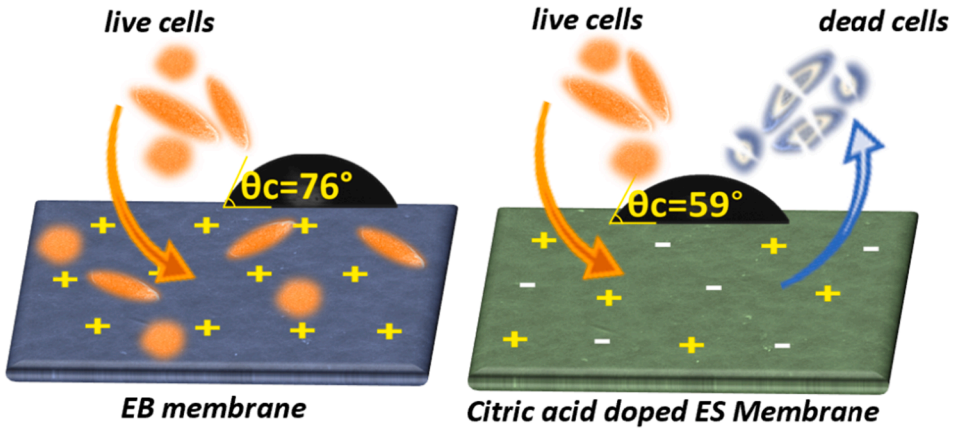

Scheme 2. Anti-adhesive properties of the pristine EB and citric acid doped ES membranes.

compared with the fresh counterpart (Fig. 7.b and 7.d). Both the antibacterial activity and leaching test results demonstrated that the citric acid doped membrane kills bacteria through contact killing mode (Scheme 4). This conclusion was further supported with the dynamic bacteria filtration studies. The change in antibiofouling property of the citric acid doped membrane during 5-cycle bacteria filtration (filtering 935 L/m^2 of *E.coli* and *S.aureus* solutions) was found negligible (Fig. 8).

In general, the inactivation of bacteria through contact-killing is described in 4 steps: Binding of antibacterial agents to cell membranes by ionic and/or hydrophobic interactions [3,108-110], damage of cell membrane, degradation of DNA and damage of intracellular compartment [111]. Although our data showed that the citric acid doped ES membrane inactivates bacteria through contact-killing mechanism, the exact bactericidal mechanism remains unclear and can be investigated as a comprehensive study in the future.

The antibacterial nanoparticles are commonly used to mitigate the biofilm formation on membrane surfaces through release-killing mechanism. However, their continuous release results in a shorter lasting period of the membrane and may cause toxic effects on the environment and human health. Citric acid has a favorable ecological profile with very low aquatic toxicity and fast biodegradability [112]. Considering a minimal amount of citric acid released into high salinity water, we can conclude that the membrane developed in this study does not pose any risk to the environment. Based on leaching and bacteria filtration tests, it can also be suggested that the anti-biofouling properties of the citric acid doped membrane can be stable in long-term filtration."

4. Conclusion

The present study aimed to enhance the anti-biofouling performance of the PANI-based UF membrane through citric acid doping. The doping was carried out with a one-step, simple filtration of acid. The doped

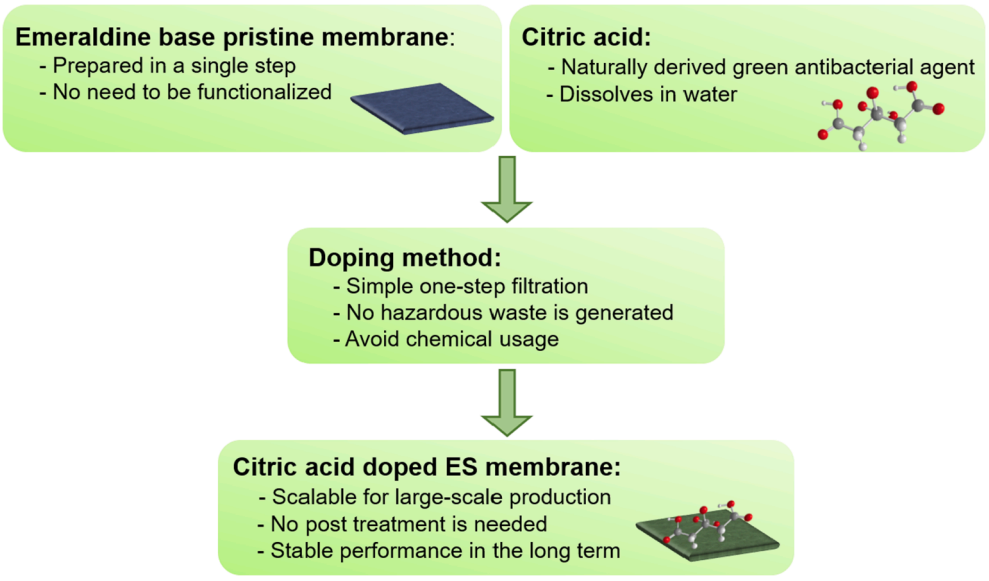

Scheme 3. Applied strategies in this study to produce greener membrane.

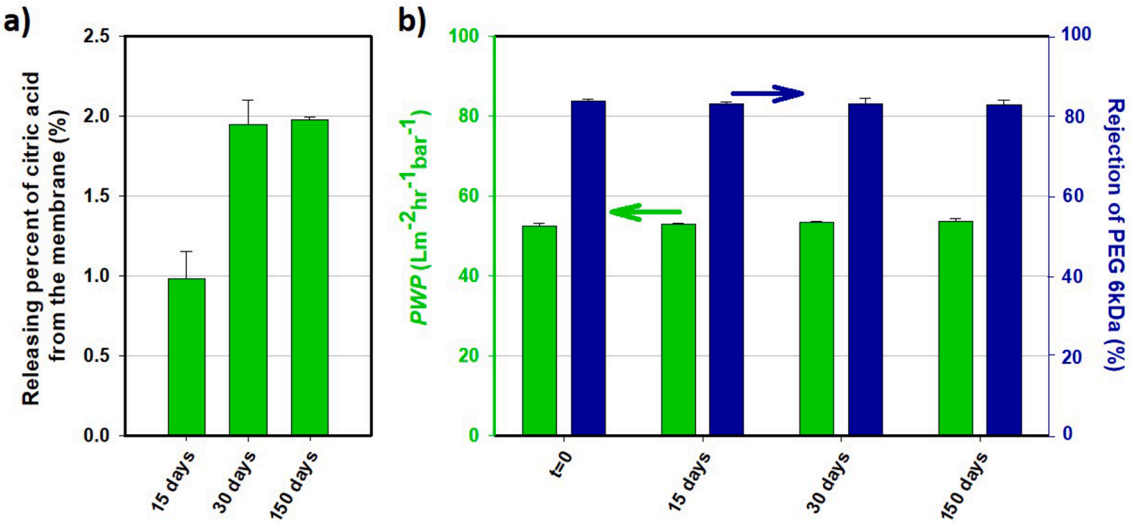

Fig. 11. Stability test results of citric acid doped ES membrane.

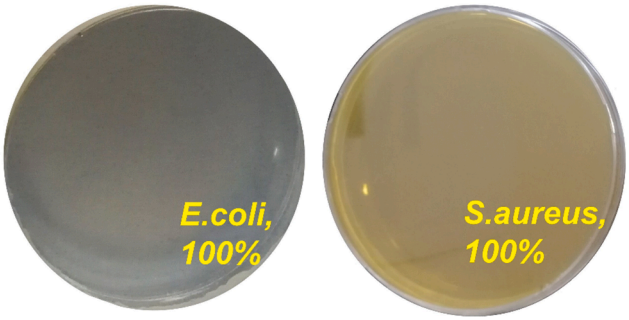

Fig. 12. Bactericidal rates within 24 hr incubation time for the citric acid doped ES membranes after 1-month storage in 1 M NaCl solution (Bacteria suspensions were diluted 100-fold, before spreading on these plates).

membrane exhibited excellent antibacterial activity against Gram-negative and Gram-positive bacteria in comparison to the pristine membrane. Improved biofouling resistance resulted from the combination of anti-adhesion and antibacterial properties. Slight flux decline observed for the doped membrane during filtration of bacteria solution was almost fully recovered after washing with PBS. However, the pristine PANI membrane could not inhibit the biofilm formation, and an intense bacterial population remained on its surface at the end of each filtration cycle followed by washing. Leaching experiments demonstrated that the doped citric acid was stable in the structure. Also, the antibacterial activity of the citric acid doped ES membrane against *E. coli* and *S.aureus* did not change after one-month storage in 1 M NaCl solution. The results suggest that the doped ES membrane has a great potential for desalination applications where the biofouling resistance and stability under high salinity are two important criteria for the membrane selection.

Due to the growing concern of global environmental pollution, green synthesis of membranes is needed to reach sustainable development goals. In this respect, we aimed to reduce the number of preparation steps by choosing the right antibacterial agent for the membrane polymer. We used a naturally derived antibacterial agent, and its minor release into the environment does not cause any toxic effect on the aquatic environment. Also, neither the antibacterial agent nor the

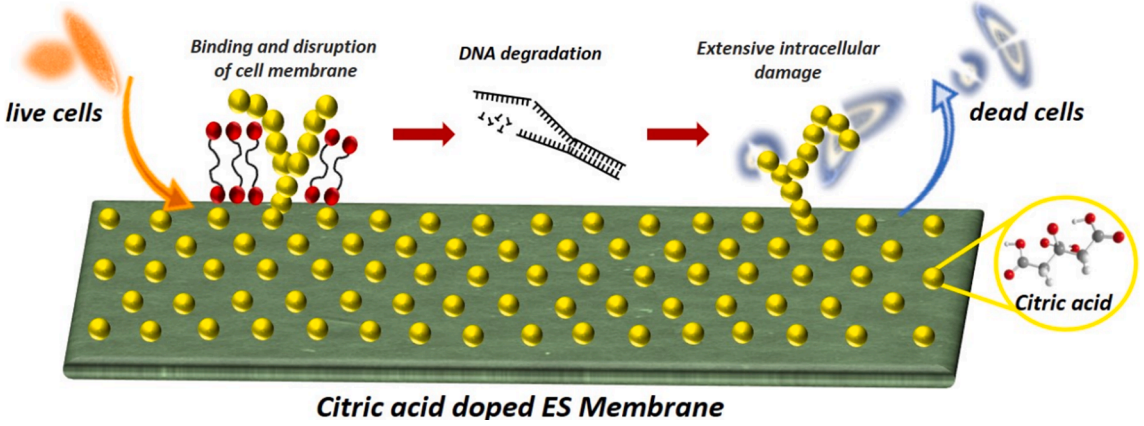

Scheme 4. Bacteria killing mechanism of the citric acid doped ES membrane.

support membrane requires functionalization before loading. These choices and the protocol adopted in this study contributed to sustainable membrane development. In addition, the scale-up of the protocol is easy for large-scale sustainable production.

CRediT authorship contribution statement

Elif Gungormus: Investigation, Methodology, Formal analysis, Data curation, Writing –original draft. **Sacide Alsoy Altinkaya:** Conceptualization, Writing – original draft, Writing – review & editing, Supervision.

Declaration of Competing Interest

The authors declare that they have no known competing financial interests or personal relationships that could have appeared to influence the work reported in this paper.

Acknowledgement

We would like to thank the Material Research Centre and Biotechnology and Bioengineering Application Research Centre at the Izmir Institute of Technology for their kind help and technical support. This research did not receive any specific grant from funding agencies in the public, commercial, or not-for-profit sectors.

References

[1] R. Komlenic, Rethinking the causes of membrane biofouling, Filtr. Sep. 47 (5) (2010) 26–28, https://doi.org/10.1016/S0015-1882(10)70211-1.
[2] X. Zhang, Z. Wang, M. Chen, J. Ma, S. Chen, Z. Wu, Membrane biofouling control using polyvinylidene fluoride membrane blended with quaternary ammonium compound assembled on carbon material, J. Membr. Sci. 539 (2017) 229–237, https://doi.org/10.1016/j.memsci.2017.06.008.
[3] X. Zhang, J. Ma, C.Y. Tang, Z. Wang, H.Y. Ng, Z. Wu, Antibiofouling polyvinylidene fluoride membrane modified by quaternary ammonium compound: Direct contact-killing versus induced indirect contact-killing, Environ. Sci. Technol. 50 (10) (2016) 5086–5093, https://doi.org/10.1021/acs.est.6b0090210.1021/acs.est.6b00902.s001.
[4] S.-Y. Wang, L.-F. Fang, B.-K. Zhu, H. Matsuyama, Enhancing the antifouling property of polymeric membrane via surface charge regulation, J. Colloid Interface Sci. 593 (2021) 315–322, https://doi.org/10.1016/j.jcis.2021.03.004.
[5] J.S. Louie, I. Pinnau, I. Ciobanu, K.P. Ishida, A. Ng, M. Reinhard, Effects of polyether–polyamide block copolymer coating on performance and fouling of reverse osmosis membranes, J. Membr. Sci 280 (1-2) (2006) 762–770, https://doi.org/10.1016/j.memsci.2006.02.041.
[6] R.A. Al-Juboori, T. Yusaf, Biofouling in RO system: Mechanisms, monitoring and controlling, Desalination 302 (2012) 1–23, https://doi.org/10.1016/j.desal.2012.06.016.
[7] R. Kumar, A.F. Ismail, Fouling control on microfiltration/ultrafiltration membranes: Effects of morphology, hydrophilicity, and charge, J. Appl. Polym. Sci. 132 (2015) 21, https://doi.org/10.1002/app.42042.
[8] J. Wang, Z. Wang, J. Wang, S. Wang, Improving the water flux and bio-fouling resistance of reverse osmosis (RO) membrane through surface modification by zwitterionic polymer, J. Membr. Sci. 493 (2015) 188–199, https://doi.org/10.1016/j.memsci.2015.06.036.
[9] Y.-F. Yang, Y. Li, Q.-L. Li, L.-S. Wan, Z.-K. Xu, Surface hydrophilization of microporous polypropylene membrane by grafting zwitterionic polymer for anti-biofouling, J. Membr. Sci. 362 (1-2) (2010) 255–264, https://doi.org/10.1016/j.memsci.2010.06.048.
[10] F. Razi, I. Sawada, Y. Ohmukai, T. Maruyama, H. Matsuyama, The improvement of antibiofouling efficiency of polyethersulfone membrane by functionalization with zwitterionic monomers, J. Membr. Sci. 401–402 (2012) 292–299, https://doi.org/10.1016/j.memsci.2012.02.020.
[11] D. Saeki, T. Tanimoto, H. Matsuyama, Anti-biofouling of polyamide reverse osmosis membranes using phosphorylcholine polymer grafted by surface-initiated atom transfer radical polymerization, Desalination 350 (2014) 21–27, https://doi.org/10.1016/j.desal.2014.07.004.
[12] C. Liu, A.F. Faria, J. Ma, M. Elimelech, Mitigation of biofilm development on thin-film composite membranes functionalized with zwitterionic polymers and silver nanoparticles, Environ. Sci. Technol. 51 (1) (2017) 182–191, https://doi.org/10.1021/acs.est.6b0379510.1021/acs.est.6b03795.s001.
[13] Y.-C. Chiang, Y. Chang, C.-J. Chuang, R.-C. Ruaan, A facile zwitterionization in the interfacial modification of low bio-fouling nanofiltration membranes, J. Membr. Sci. 389 (2012) 76–82, https://doi.org/10.1016/j.memsci.2011.10.017.
[14] H. Karkhanechi, R. Takagi, H. Matsuyama, Enhanced antibiofouling of RO membranes via polydopamine coating and polyzwitterion immobilization, Desalination 337 (2014) 23–30, https://doi.org/10.1016/j.desal.2014.01.007.
[15] Y. Zhang, Z. Wang, W. Lin, H. Sun, L. Wu, S. Chen, A facile method for polyamide membrane modification by poly(sulfobetaine methacrylate) to improve fouling resistance, J. Membr. Sci. 446 (2013) 164–170, https://doi.org/10.1016/j.memsci.2013.06.013.
[16] R. Bernstein, S. Belfer, V. Freger, Bacterial attachment to RO membranes surface-modified by concentration-polarization-enhanced graft polymerization, Environ. Sci. Technol. 45 (14) (2011) 5973–5980, https://doi.org/10.1021/es1043694.
[17] J. Meng, Z. Cao, L. Ni, Y. Zhang, X. Wang, X. Zhang, E. Liu, A novel salt-responsive TFC RO membrane having superior antifouling and easy-cleaning properties, J. Membr. Sci. 461 (2014) 123–129, https://doi.org/10.1016/j.memsci.2014.03.017.
[18] Y.-C. Chiang, Y. Chang, A. Higuchi, W.-Y. Chen, R.-C. Ruaan, Sulfobetaine-grafted poly(vinylidene fluoride) ultrafiltration membranes exhibit excellent antifouling property, J. Membr. Sci. 339 (1-2) (2009) 151–159, https://doi.org/10.1016/j.memsci.2009.04.044.
[19] Z. Zhang, S. Chen, Y. Chang, S. Jiang, Surface grafted sulfobetaine polymers via atom transfer radical polymerization as superlow fouling coatings, J. Phys. Chem. B 110 (22) (2006) 10799–10804, https://doi.org/10.1021/jp057266i.
[20] M. Ben-Sasson, K.R. Zodrow, Q.i. Genggeng, Y. Kang, E.P. Giannelis, M. Elimelech, Surface functionalization of thin-film composite membranes with copper nanoparticles for antimicrobial surface properties, Environ. Sci. Technol. 48 (1) (2014) 384–393, https://doi.org/10.1021/es404232s.
[21] K. Zodrow, L. Brunet, S. Mahendra, D. Li, A. Zhang, Q. Li, P.J.J. Alvarez, Polysulfone ultrafiltration membranes impregnated with silver nanoparticles show improved biofouling resistance and virus removal, Water Res. 43 (3) (2009) 715–723, https://doi.org/10.1016/j.watres.2008.11.014.
[22] D.Y. Koseoglu-Imer, B. Kose, M. Altinbas, I. Koyuncu, The production of polysulfone (PS) membrane with silver nanoparticles (AgNP): Physical properties, filtration performances, and biofouling resistances of membranes, J. Membr. Sci. 428 (2013) 620–628, https://doi.org/10.1016/j.memsci.2012.10.046.
[23] X. Li, R. Pang, J. Li, X. Sun, J. Shen, W. Han, L. Wang, In situ formation of Ag nanoparticles in PVDF ultrafiltration membrane to mitigate organic and bacterial fouling, Desalination 324 (2013) 48–56, https://doi.org/10.1016/j.desal.2013.05.021.
[24] I. Sawada, R. Fachrul, T. Ito, Y. Ohmukai, T. Maruyama, H. Matsuyama, Development of a hydrophilic polymer membrane containing silver nanoparticles

with both organic antifouling and antibacterial properties, J. Membr. Sci. 387–388 (2012) 1–6, https://doi.org/10.1016/j.memsci.2011.06.020.
[25] S.F. Seyedpour, A. Rahimpour, G. Najafpour, Facile in-situ assembly of silver-based MOFs to surface functionalization of TFC membrane: A novel approach toward long-lasting biofouling mitigation, J. Membr. Sci. 573 (2019) 257–269, https://doi.org/10.1016/j.memsci.2018.12.016.
[26] J.A. Prince, S. Bhuvana, V. Anbharasi, N. Ayyanar, K.V.K. Boodhoo, G. Singh, Self-cleaning Metal Organic Framework (MOF) based ultra filtration membranes - A solution to bio-fouling in membrane separation processes, Sci. Rep. 4 (2014) 6555, https://doi.org/10.1038/srep06555.
[27] Z. Zeng, D. Yu, Z. He, J. Liu, F.X. Xiao, Y. Zhang, R. Wang, D. Bhattacharyya, T. T. Tan, Graphene oxide quantum dots covalently functionalized PVDF membrane with significantly-enhanced bactericidal and antibiofouling performances, Sci. Rep. 6 (2016) 20142, https://doi.org/10.1038/srep20142.
[28] A. Anand, B. Unnikrishnan, S.-C. Wei, C.P. Chou, L.-Z. Zhang, C.-C. Huang, Graphene oxide and carbon dots as broad-spectrum antimicrobial agents – a mini review, Nanoscale Horiz. 4 (1) (2019) 117–137, https://doi.org/10.1039/C8NH00174J.
[29] Q. Liu, G.-R. Xu, Graphene oxide (GO) as functional material in tailoring polyamide thin film composite (PA-TFC) reverse osmosis (RO) membranes, Desalination 394 (2016) 162–175, https://doi.org/10.1016/j.desal.2016.05.017.
[30] R. Das, M.E. Ali, S.B.A. Hamid, S. Ramakrishna, Z.Z. Chowdhury, Carbon nanotube membranes for water purification: A bright future in water desalination, Desalination 336 (2014) 97–109, https://doi.org/10.1016/j.desal.2013.12.026.
[31] D.L. Zhao, T.-S. Chung, Applications of carbon quantum dots (CQDs) in membrane technologies: A review, Water Res. 147 (2018) 43–49, https://doi.org/10.1016/j.watres.2018.09.040.
[32] H.M. Hegab, L. Zou, Graphene oxide-assisted membranes: Fabrication and potential applications in desalination and water purification, J. Membr. Sci. 484 (2015) 95–106, https://doi.org/10.1016/j.memsci.2015.03.011.
[33] W. Zhang, W. Cheng, E. Ziemann, A. Be'er, X. Lu, M. Elimelech, R. Bernstein, Functionalization of ultrafiltration membrane with polyampholyte hydrogel and graphene oxide to achieve dual antifouling and antibacterial properties, J. Membr. Sci. 565 (2018) 293–302, https://doi.org/10.1016/j.memsci.2018.08.017.
[34] X. Zhang, Z. Wang, M. Chen, M. Liu, Z. Wu, Polyvinylidene fluoride membrane blended with quaternary ammonium compound for enhancing anti-biofouling properties: Effects of dosage, J. Membr. Sci. 520 (2016) 66–75, https://doi.org/10.1016/j.memsci.2016.07.048.
[35] Y. Wen, X.R. Zhang, M. Chen, Z.C. Wu, Z.W. Wang, Characterization of antibiofouling behaviors of PVDF membrane modified by quaternary ammonium compound - combined use of QCM-D, FCM, and CLSM, J. Water Reuse Desalination 9 (2019) 18–30, https://doi.org/10.2166/wrd.2018.017.
[36] M. Ping, X. Zhang, M. Liu, Z. Wu, Z. Wang, Surface modification of polyvinylidene fluoride membrane by atom-transfer radical-polymerization of quaternary ammonium compound for mitigating biofouling, J. Membr. Sci. 570–571 (2019) 286–293, https://doi.org/10.1016/j.memsci.2018.10.070.
[37] F. Razi, I. Sawada, Y. Ohmukai, T. Maruyama, H. Matsuyama, Surface functionalization by grafting (2-Dimethylamino)ethyl methacrylate methyl chloride quaternary salt (DMAEMAq) onto hollow fiber polyethersulfone (PES) membranes for improvement of antibiofouling properties, Solvent Extr. Res. Dev. Jpn. 19 (2012) 101–115. https://doi.org/10.15261/serdj.19.101.
[38] C. Wang, Z. Li, L. Cao, B. Cheng, A superhydrophilic and anti-biofouling polyphenylene sulfide microporous membrane with quaternary ammonium salts, Macromol. Res. 26 (9) (2018) 800–807, https://doi.org/10.1007/s13233-018-6108-y.
[39] C. Wu, Z. Wang, S. Liu, Z. Xie, H. Chen, X. Lu, Simultaneous permeability, selectivity and antibacterial property improvement of PVC ultrafiltration membranes via in-situ quaternization, J. Membr. Sci. 548 (2018) 50–58, https://doi.org/10.1016/j.memsci.2017.11.008.
[40] X.R. Zhang, Z.W. Wang, C.Y.Y. Tang, J.X. Ma, M.X. Liu, M. Ping, M. Chen, Z. C. Wu, Modification of microfiltration membranes by alkoxysilane polycondensation induced quaternary ammonium compounds grafting for biofouling mitigation, J. Membr. Sci. 549 (2018) 165–172, https://doi.org/10.1016/j.memsci.2017.12.004.
[41] Y. Kakihana, L. Cheng, L.-F. Fang, S.-Y. Wang, S. Jeon, D. Saeki, S. Rajabzadeh, H. Matsuyama, Preparation of positively charged PVDF membranes with improved antibacterial activity by blending modification: Effect of change in membrane surface material properties, Colloids Surf, A Physicochem Eng Asp. 533 (2017) 133–139, https://doi.org/10.1016/j.colsurfa.2017.08.039.
[42] J.-W. Xu, Y. Wang, Y.-F. Yang, X.-Y. Ye, K. Yao, J. Ji, Z.-K. Xu, Effects of quaternization on the morphological stability and antibacterial activity of electrospun poly(DMAEMA-co-AMA) nanofibers, Colloids Surf. B Biointerfaces 133 (2015) 148–155, https://doi.org/10.1016/j.colsurfb.2015.06.002.
[43] A. Cihanoğlu, S.A. Altinkaya, A facile route to the preparation of antibacterial polysulfone-sulfonated polyethersulfone ultrafiltration membranes using a cationic surfactant cetyltrimethylammonium bromide, J. Membr. Sci. 594 (2020) 117438, https://doi.org/10.1016/j.memsci.2019.117438.
[44] J. Shen, S. Shahid, A. Sarihan, D.A. Patterson, E.A.C. Emanuelsson, Effect of polyacid dopants on the performance of polyaniline membranes in organic solvent nanofiltration, Sep. Purif. Technol. 204 (2018) 336–344, https://doi.org/10.1016/j.seppur.2018.04.034.
[45] J.J. Smith, B.E. Wayman, An evaluation of the antimicrobial effectiveness of citric acid as a root canal irrigant, J. Endod. 12 (2) (1986) 54–58, https://doi.org/10.1016/S0099-2399(86)80128-5.
[46] M. GEORGOPOULOU, E. KONTAKIOTIS, M. NAKOU, Evaluation of the antimicrobial effectiveness of citric acid and sodium hypochlorite on the anaerobic flora of the infected root canal, Int. Endod. J. 27 (3) (1994) 139–143, https://doi.org/10.1111/iej.1994.27.issue-310.1111/j.1365-2591.1994.tb00243.x.
[47] L.-C. Su, Z. Xie, Y. Zhang, K.T. Nguyen, J. Yang, Study on the Antimicrobial properties of citrate-based biodegradable polymers, Front Bioeng, 23 23, Biotechnol. 2 (2014), https://doi.org/10.3389/fbioe.2014.00023.
[48] E.T. Kang, K.G. Neoh, K.L. Tan, Polyaniline: A polymer with many interesting intrinsic redox states, Prog. Polym. Sci. 23 (1998) 277–324, https://doi.org/10.1016/S0079-6700(97)00030-0.
[49] E.T. Kang, K.G. Neoh, S.H. Khor, K.L. Tan, B.T.G. Tan, X.p.s. studies of charge transfer interactions in some polyaniline complexes, Polymer 31 (2) (1990) 202–207, https://doi.org/10.1016/0032-3861(90)90106-9.
[50] S. Zhao, L. Huang, T. Tong, W. Zhang, Z. Wang, J. Wang, S. Wang, Antifouling and antibacterial behavior of polyethersulfone membrane incorporating polyaniline@silver nanocomposites, Environ. Sci. Water Res. Technol. 3 (4) (2017) 710–719, https://doi.org/10.1039/C6EW00332J.
[51] M. Khajouei, M. Jahanshahi, M. Peyravi, Biofouling mitigation of TFC membrane by in-situ grafting of PANI/Cu couple nanoparticle, J. Taiwan Inst. Chem. Eng. 85 (2018) 237–247, https://doi.org/10.1016/j.jtice.2018.01.027.
[52] Z.A. Boeva, V.G.J.P.S.S.C. Sergeyev, Polyaniline: Synthesis, properties, and application, Polym. Sci. Ser. C 56 (2014) 144-153. https://doi.org/10.1134/S1811238214010032.
[53] K.A. Ibrahim, Synthesis and characterization of polyaniline and poly(aniline-co-o-nitroaniline) using vibrational spectroscopy, Arab. J. Chem. 10 (2017) S2668–S2674, https://doi.org/10.1016/j.arabjc.2013.10.010.
[54] E. C. Gomes, M. A. S. Oliveira, Chemical polymerization of aniline in hydrochloric acid (HCl) and formic acid (HCOOH) media. Differences between the two synthesized polyanilines, Am. J. Polym. Sci. 2 (2) (2012) 5–13, https://doi.org/10.5923/j.ajps.20120202.02.
[55] Elif Gungormus, Sacide Alsoy Altinkaya, A high-performance acid-resistant polyaniline based ultrafiltration membrane: Application in the production of aluminium sulfate powder from alumina sol, Chem. Eng. J. 389 (2020) 124393, https://doi.org/10.1016/j.cej.2020.124393.
[56] Supakorn Atchariyawut, Chunsheng Feng, Rong Wang, Ratana Jiraratananon, D. T. Liang, Effect of membrane structure on mass-transfer in the membrane gas–liquid contacting process using microporous PVDF hollow fibers, J. Membr. Sci. 285 (1-2) (2006) 272–281, https://doi.org/10.1016/j.memsci.2006.08.029.
[57] T.-Y. Liu, L.-X. Bian, H.-G. Yuan, B. Pang, Y.-K. Lin, Y. Tong, B. Van der Bruggen, X.-L. Wang, Fabrication of a high-flux thin film composite hollow fiber nanofiltration membrane for wastewater treatment, J. Membr. Sci. 478 (2015) 25–36, https://doi.org/10.1016/j.memsci.2014.12.029.
[58] J. Lin, W. Ye, M.C. Baltaru, Y.P. Tang, N.J. Bernstein, P. Gao, S. Balta, M. Vlad, A. Volodin, A. Sotto, P. Luis, A.L. Zydney, B.V. Bruggen, Tight ultrafiltration membranes for enhanced separation of dyes and Na2SO4 during textile wastewater treatment, J. Membr. Sci. 514 (2016) 217–228, https://doi.org/10.1016/j.memsci.2016.04.057.
[59] S Singh, K.C Khulbe, T Matsuura, P Ramamurthy, Membrane characterization by solute transport and atomic force microscopy, J. Membr. Sci. 142 (1) (1998) 111–127, https://doi.org/10.1016/S0376-7388(97)00329-3.
[60] G. Dognani, P. Hadi, H. Ma, F.C. Cabrera, A.E. Job, D.L.S. Agostini, B.S. Hsiao, Effective chromium removal from water by polyaniline-coated electrospun adsorbent membrane, Chem. Eng. J. 372 (2019) 341–351, https://doi.org/10.1016/j.cej.2019.04.154.
[64] LUIZ EDUARDO SILVA, PEDRO IVO CUNHA CLARO, RAFAELA CRISTINA SANFELICE, MÁRIO GUIMARÃES JÚNIOR, JULIANO ELVIS DE OLIVEIRA, JÚLIO CÉSAR UGUCIONI, DANIEL SOUZA CORREA, GUSTAVO HENRIQUE DENZIN TONOLI, Cellulose nanofibrils modification with polyaniline aiming at enhancing electrical properties for application in flexible electronics, Cellul. Chem. Technol. 53 (7-8) (2019) 775–786.
[65] N.T. Thuy, D.L. Minh, Size effect on the structural and magnetic properties of nanosized Perovskite $LaFeO_3$ prepared by different methods, Adv. Mater. Sci. Eng. 380306 (2012), https://doi.org/10.1155/2012/380306.
[66] V. Rajasekharan, S. Viswanathan, P. Manisankar, Electrochemical evaluation of anticorrosive performance of organic acid doped polyaniline based coatings, Int. J. Electrochem. Sci. 8 (2013) 11327–11336.
[67] C CAUSSERAND, S ROUAIX, A AKBARI, P AIMAR, Improvement of a method for the characterization of ultrafiltration membranes by measurements of tracers retention, J. Membr. Sci 238 (1-2) (2004) 177–190, https://doi.org/10.1016/j.memsci.2004.04.003.
[68] Fang Xu, Yang Song, Mingjie Wei, Yong Wang, Water flow through interlayer channels of two-dimensional materials with various hydrophilicities, J. Phys. Chem. C 122 (27) (2018) 15772–15779, https://doi.org/10.1021/acs.jpcc.8b0471910.1021/acs.jpcc.8b04719.s001.
[69] Y. Liu, X. Chen, High permeability and salt rejection reverse osmosis by a zeolite nano-membrane, Phys. Chem. Chem. Phys. 15 (2013) 6817–6824, https://doi.org/10.1039/C3CP43854F.
[70] J. Delcour, T. Ferain, M. Deghorain, E. Palumbo, P. Hols, The biosynthesis and functionality of the cell-wall of lactic acid bacteria, Antonie van Leeuwenhoek 76 (1999) 159–184.
[71] Terry J. Beveridge, Structures of gram-negative cell walls and their derived membrane vesicles, J. Bacteriol. 181 (16) (1999) 4725–4733, https://doi.org/10.1128/JB.181.16.4725-4733.1999.
[72] J. Wang, H. Sun, X. Gao, C. Gao, Enhancing antibiofouling performance of polysulfone (PSf) membrane by photo-grafting of capsaicin derivative and acrylic

acid, Appl. Surf. Sci. 317 (2014) 210–219, https://doi.org/10.1016/j.apsusc.2014.08.102.
[73] Q. Wang, J. Wang, X. Gao, H. Yu, Z. Ma, Y. Zhang, C. Gao, Antibiofouling polysulfone ultrafiltration membranes via surface grafting of capsaicin derivatives, Water Sci. Technol. 79 (2019) 1821–1832, https://doi.org/10.2166/wst.2019.182.
[74] Biao Kang, Ying-Dong Li, Jie Liang, Xi Yan, Jun Chen, Wan-Zhong Lang, Novel PVDF hollow fiber ultrafiltration membranes with antibacterial and antifouling properties by embedding N-halamine functionalized multi-walled carbon nanotubes (MWNTs), RSC Adv. 6 (3) (2016) 1710–1721, https://doi.org/10.1039/C5RA24804C.
[75] Y. Chen, Y. Zhang, H. Zhang, J. Liu, C. Song, Biofouling control of halloysite nanotubes-decorated polyethersulfone ultrafiltration membrane modified with chitosan-silver nanoparticles, Chem. Eng. J. 228 (2013) 12–20, https://doi.org/10.1016/j.cej.2013.05.015.
[76] Q. Yu, Y. Qin, M. Han, F. Pan, L. Han, X. Yin, Z. Chen, L. Wang, H. Wang, Preparation and characterization of solvent-free fluids reinforced and plasticized polylactic acid fibrous membrane, Int. J. Biol. Macromol. 161 (2020) 122–131, https://doi.org/10.1016/j.ijbiomac.2020.06.027.
[77] S. Hou, X. Dong, J. Zhu, J. Zheng, W. Bi, S. Li, S. Zhang, Preparation and characterization of an antibacterial ultrafiltration membrane with N-chloramine functional groups, J. Colloid Interface Sci. 496 (2017) 391–400, https://doi.org/10.1016/j.jcis.2017.01.054.
[78] B. Rodríguez, D. Oztürk, M. Rosales, M. Flores, A.J.J.o.M.S. García, Antibiofouling thin-film composite membranes (TFC) by in situ formation of Cu-(m-phenylenediamine) oligomer complex, Biomaterials 53 (2018) 6325-6338. https://doi.org/10.1007/s10853-018-2039-4.
[79] B.P. Tripathi, N.C. Dubey, S. Choudhury, F. Simon, M. Stamm, Antifouling and antibiofouling pH responsive block copolymer based membranes by selective surface modification, J. Mater. Chem. B 1 (2013) 3397–3409, https://doi.org/10.1039/C3TB20386G.
[80] X.-F. Sun, J. Qin, P.-F. Xia, B.-B. Guo, C.-M. Yang, C. Song, S.-G. Wang, Graphene oxide–silver nanoparticle membrane for biofouling control and water purification, Chem. Eng. J. 281 (2015) 53–59, https://doi.org/10.3390/nano10030454.
[81] X. Wang, S. Jing, Y. Liu, S. Liu, Y. Tan, Diblock copolymer containing bioinspired borneol and dopamine moieties: Synthesis and antibacterial coating applications, Polymer 116 (2017) 314–323, https://doi.org/10.1016/j.polymer.2017.03.078.
[82] L. Yu, Y. Zhang, B. Zhang, J. Liu, H. Zhang, C. Song, Preparation and characterization of HPEI-GO/PES ultrafiltration membrane with antifouling and antibacterial properties, J. Membr. Sci. 447 (2013) 452–462, https://doi.org/10.1016/j.memsci.2013.07.042.
[83] Yi Feng, Xiaocheng Lin, Huazhen Li, Lizhong He, Tam Sridhar, Akkihebbal K Suresh, Jayesh Bellare, Huanting Wang, Synthesis and characterization of chitosan-grafted BPPO ultrafiltration composite membranes with enhanced antifouling and antibacterial properties, Ind. Eng. Chem. Res. 53 (39) (2014) 14974–14981, https://doi.org/10.1021/ie502599p.
[84] H.-T. Wang, D. Ao, M.-C. Lu, N. Chang, Alteration of the morphology of polyvinylidene fluoride membrane by incorporating MOF-199 nanomaterials for improving water permeation with antifouling and antibacterial property, J. Chin. Chem. Soc. 67 (2020) 1807–1817, https://doi.org/10.1002/jccs.202000055.
[85] L.L. Zhang, Y.Y. Tang, X.H. Jiang, L.M. Yu, C.Y. Wang, Highly dual antifouling and antibacterial ultrafiltration membranes modified with silane coupling agent and capsaicin-mimic moieties, Polymers 12 (2020) 17, https://doi.org/10.3390/polym12020412.
[86] M.Y. Hu, Z.Y. Cui, J. Li, L. Zhang, Y.H. Mo, D.S. Dlamini, H. Wang, B.Q. He, J. X. Li, H. Matsuyama, Ultra-low graphene oxide loading for water permeability, antifouling and antibacterial improvement of polyethersulfone/sulfonated polysulfone ultrafiltration membranes, J. Colloid Interface Sci. 552 (2019) 319–331, https://doi.org/10.1016/j.jcis.2019.05.065.
[87] F.A.A. Ali, J. Alam, A.K. Shukla, M. Alhoshan, M.A. Ansari, W.A. Al-Masry, S. Rehman, M. Alam, Evaluation of antibacterial and antifouling properties of silver-loaded GO polysulfone nanocomposite membrane against Escherichia coli, Staphylococcus aureus, and BSA protein, React. Funct. Polym. 140 (2019) 136–147, https://doi.org/10.1016/j.reactfunctpolym.2019.04.019.
[88] Wei Zhang, Yang Yang, Eric Ziemann, Avraham Be'er, Muhammad Y. Bashouti, Menachem Elimelech, Roy Bernstein, One-step sonochemical synthesis of a reduced graphene oxide – ZnO nanocomposite with antibacterial and antibiofouling properties, Environ. Sci, Nano 6 (10) (2019) 3080–3090, https://doi.org/10.1039/C9EN00753A.
[89] Ranjith Kumar Manoharan, Sivasankaran Ayyaru, Young-Ho Ahn, Auto-cleaning functionalization of the polyvinylidene fluoride membrane by the biocidal oxine/TiO2 nanocomposite for anti-biofouling properties, New J. Chem. 44 (3) (2020) 807–816, https://doi.org/10.1039/C9NJ05300J.
[90] Mohit Chaudhary, Abhijit Maiti, Fe-Al-Mn@chitosan based metal oxides blended cellulose acetate mixed matrix membrane for fluoride decontamination from water: Removal mechanisms and antibacterial behavior, J. Membr. Sci. 611 (2020) 118372, https://doi.org/10.1016/j.memsci.2020.118372.
[91] Hanxiang Guo, Zhaofeng Wang, Yang Liu, Pengfei Huo, Jiyou Gu, Fangbo Zhao, Synthesis and characterization of novel zwitterionic poly(aryl ether oxadiazole) ultrafiltration membrane with good antifouling and antibacterial properties, J. Membr. Sci. 611 (2020) 118337, https://doi.org/10.1016/j.memsci.2020.118337.
[92] Shuge Peng, Yamin Chen, Xiaopan Jin, Weiwei Lu, Minglei Gou, Xuefeng Wei, Jingpei Xie, Polyimide with half encapsulated silver nanoparticles grafted ceramic composite membrane: Enhanced silver stability and lasting anti-biofouling performance, J. Membr. Sci. 611 (2020) 118340, https://doi.org/10.1016/j.memsci.2020.118340.
[93] S.Y. Zhou, J. Gao, J.Y. Zhu, D.L. Peng, Y.M. Zhang, Y.T. Zhang, Self-cleaning, antibacterial mixed matrix membranes enabled by photocatalyst Ti-MOFs for efficient dye removal, J. Membr. Sci. 610 (2020) 10, https://doi.org/10.1016/j.memsci.2020.118219.
[94] M.B. Gohain, R.R. Pawar, S. Karki, A. Hazarika, S. Hazarika, P.G. Ingole, Development of thin film nanocomposite membrane incorporated with mesoporous synthetic hectorite and MSH@UiO-66-NH2 nanoparticles for efficient targeted feeds separation, and antibacterial performance, J. Membr. Sci. 609 (2020) 17, https://doi.org/10.1016/j.memsci.2020.118212.
[95] S.J. Yang, T.H. Wang, R. Tang, Q.L. Yan, W.Q. Tian, L.P. Zhang, Enhanced permeability, mechanical and antibacterial properties of cellulose acetate ultrafiltration membranes incorporated with lignocellulose nanofibrils, Int. J. Biol. Macromol. 151 (2020) 159–167, https://doi.org/10.1016/j.ijbiomac.2020.02.124.
[96] N. Ahmad, A. Samavati, N. Nordin, J. Jaafar, A.F. Ismail, N. Malek, Enhanced performance and antibacterial properties of amine-functionalized ZIF-8-decorated GO for ultrafiltration membrane, Sep. Purif. Technol. 239 (2020) 13, https://doi.org/10.1016/j.seppur.2020.116554.
[97] S. Krishnan, C.J. Weinman, C.K. Ober, Advances in polymers for anti-biofouling surfaces, J. Mater. Chem. 18 (2008) 3405–3413, https://doi.org/10.1039/B801491D.
[98] M.R. Hibbs, L.K. McGrath, S. Kang, A. Adout, S.J. Altman, M. Elimelech, C. J. Cornelius, Designing a biocidal reverse osmosis membrane coating: Synthesis and biofouling properties, Desalination 380 (2016) 52–59, https://doi.org/10.1016/j.desal.2015.11.017.
[99] Yekyung Kim, Dipak Rana, Takeshi Matsuura, Wook-Jin Chung, Towards antibiofouling ultrafiltration membranes by blending silver containing surface modifying macromolecules, Chem. Commun. 48 (5) (2012) 693–695, https://doi.org/10.1039/C1CC16217A.
[100] A.B. Koltuniewicz, R.W. Field, T.C. Arnot, Cross-flow and dead-end microfiltration of oily-water emulsion. Part I: Experimental study and analysis of flux decline, J. Membr. Sci. 102 (1995) 193–207, https://doi.org/10.1016/0376-7388(94)00320-X.
[101] Gourav Mishra, Mausumi Mukhopadhyay, Flux improvement, rejection, surface energy and antibacterial properties of synthesized TiO2-Mo.HNTs/PVC nanocomposite ultrafiltration membranes, New J. Chem. 41 (24) (2017) 15049–15057, https://doi.org/10.1039/C7NJ02774E.
[102] K. Samree, P.-U. Srithai, P. Kotchaplai, P. Thuptimdang, P. Painmanakul, M. Hunsom, S. Sairiam, Enhancing the antibacterial properties of PVDF membrane by hydrophilic surface modification using titanium dioxide and silver nanoparticles, Membranes 10 (2020) 289, https://doi.org/10.3390/membranes10100289.
[103] J. Li, X. Liu, J. Lu, Y. Wang, G. Li, F. Zhao, Anti-bacterial properties of ultrafiltration membrane modified by graphene oxide with nano-silver particles, J. Colloid Interface Sci. 484 (2016) 107–115, https://doi.org/10.1016/j.jcis.2016.08.063.
[104] S.V. Patwardhan, J.R.H. Manning, M. Chiacchia, Bioinspired synthesis as a potential green method for the preparation of nanomaterials: Opportunities and challenges, Curr. Opin. Green Sustain. Chem. 12 (2018) 110–116, https://doi.org/10.1016/j.cogsc.2018.08.004.
[105] Munmun Mukherjee, Sirshendu De, Antibacterial polymeric membranes: a short review, Environ. Sci. Water Res. Technol. 4 (8) (2018) 1078–1104, https://doi.org/10.1039/C8EW00206A.
[106] P. Makvandi, S. Iftekhar, F. Pizzetti, A. Zarepour, E.N. Zare, M. Ashrafizadeh, T. Agarwal, V.V.T. Padil, R. Mohammadinejad, M. Sillanpaa, T.K. Maiti, G. Perale, A. Zarrabi, F. Rossi, Functionalization of polymers and nanomaterials for water treatment, food packaging, textile and biomedical applications: a review, Environ. Chem. Lett. 19 (2021) 583-611. https://doi.org/10.1007/s10311-020-01089-4.
[107] Evan Spruijt, Sebastiaan A. van den Berg, Martien A. Cohen Stuart, Jasper van der Gucht, van der Gucht, Direct measurement of the strength of single ionic bonds between hydrated charges, ACS Nano 6 6 (6) (2012) 5297–5303, https://doi.org/10.1021/nn301097y.
[108] S. Nagandran, P.S. Goh, A.F. Ismail, T.W. Wong, W.R.Z. Binti Wan Dagang, The recent progress in modification of polymeric membranes using organic macromolecules for water treatment, Symmetry 12 (2020) 239. https://doi.org/10.3390/sym12020239.
[109] Paresh Kumar Samantaray, Giridhar Madras, Suryasarathi Bose, The key role of modifications in biointerfaces toward rendering antibacterial and antifouling properties in polymeric membranes for water remediation: A critical assessment, Adv. Sustain. Syst 3 (10) (2019) 1900017, https://doi.org/10.1002/adsu.v3.1010.1002/adsu.201900017.
[110] Y. Wen, Y. Chen, Z. Wu, M. Liu, Z. Wang, Thin-film nanocomposite membranes incorporated with water stable metal-organic framework CuBTTri for mitigating biofouling, J. Membr. Sci 582 (2019) 289–297, https://doi.org/10.1016/j.memsci.2019.04.016.
[111] Marco Zeiger, Marc Solioz, Hervais Edongué, Eduard Arzt, Andreas S. Schneider, Surface structure influences contact killing of bacteria by copper, MicrobiologyOpen 3 (3) (2014) 327–332, https://doi.org/10.1002/mbo3.2014.3.issue-310.1002/mbo3.170.
[112] Johannes Tolls, Harald Berger, Adolf Klenk, Michael Meyberg, Rainer Müller, Klaus Rettinger, Josef Steber, Environmental safety aspects of personal care products–a European perspective, Environ. Toxicol. Chem. 28 (12) (2009) 2485, https://doi.org/10.1897/09-104.110.1897/09-104.S1.

Further reading

[61] S. Wang, F. Liu, C. Gao, T. Wan, L. Wang, L. Wang, L. Wang, Enhancement of the thermoelectric property of nanostructured polyaniline/carbon nanotube composites by introducing pyrrole unit onto polyaniline backbone via a sustainable method, Chem. Eng. J. 370 (2019) 322–329, https://doi.org/10.1016/j.cej.2019.03.155.

[62] Miroslava Trchová, Ivana Šeděnková, Eva Tobolková, Jaroslav Stejskal, FTIR spectroscopic and conductivitystudy of the thermal degradation of polyaniline films, Polym. Degrad. Stab. 86 (1) (2004) 179–185, https://doi.org/10.1016/j.polymdegradstab.2004.04.011.

[63] X. Huang, B.T. McVerry, C. Marambio-Jones, M.C.Y. Wong, E.M.V. Hoek, R.B. Kaner, Novel chlorine resistant low-fouling ultrafiltration membrane based on a hydrophilic polyaniline derivative, J. Mater. Chem. A 3 (2015) 8725–8733. https://doi.org/10.1039/C5TA00900F.